
Vulnerable Agent Identification in Large-Scale Multi-Agent Reinforcement Learning

Simin Li
SKLSDE Lab
Beihang University
lisiminsimon@buaa.edu.cn

Zheng Yuwei
School of Computer Science and Engineering
Beihang University
neozhengyuwei@gmail.com

Zihao Mao
Institute of Artificial Intelligence
Beihang University
zihaomao@buaa.edu.cn

Linhao Wang
School of Computer Science and Engineering
Beihang University
linhao.wang@buaa.edu.cn

Ruixiao Xu
School of Computer Science and Engineering
Beihang University
xuruixiao@buaa.edu.cn

Chengdong Ma
Institute of Artificial Intelligence
Peking University
machengdong@stu.xmu.edu.cn

Xin Yu
Institute of automation
Chinese academy of science
nlsdeyuxin@buaa.edu.cn

Yuqing Ma
School of Computer Science and Engineering
Beihang University
yuqingma@buaa.edu.cn

Qi Dou
Department of Computer Science and Engineering
The Chinese University of Hong Kong qidou@cuhk.edu.hk

Xin Wang
Institute of Artificial Intelligence
Beihang University
wangxin_1993@buaa.edu.cn

Jie Luo
School of Computer Science and Engineering
Beihang University
luojie@buaa.edu.cn

Bo An
College of Computing and Data Science
Nanyang Technological University
boan@ntu.edu.sg

Yaodong Yang
Institute of Artificial Intelligence & BigAI
Peking University
yaodong.yang@pku.edu.cn

Weifeng Lv
School of Computer Science and Engineering
Beihang University
lwf@buaa.edu.cn

Xianglong Liu*
School of Computer Science and Engineering
Beihang University
xlliu@buaa.edu.cn

Abstract

*Corresponding Author

Partial agent failure becomes inevitable when systems scale up, making it crucial to identify the subset of agents whose compromise would most severely degrade overall performance. In this paper, we study this Vulnerable Agent Identification (VAI) problem in large-scale multi-agent reinforcement learning (MARL). We frame VAI as a Hierarchical Adversarial Decentralized Mean Field Control (HAD-MFC), where the upper level involves an NP-hard combinatorial task of selecting the most vulnerable agents, and the lower level learns worst-case adversarial policies for these agents using mean-field MARL. The two problems are coupled together, making HAD-MFC difficult to solve. To solve this, we first decouple the hierarchical process by Fenchel-Rockafellar transform, resulting a regularized mean-field Bellman operator for upper level that enables independent learning at each level, thus reducing computational complexity. We then reformulate the upper-level combinatorial problem as a MDP with dense rewards from our regularized mean-field Bellman operator, enabling us to sequentially identify the most vulnerable agents by greedy and RL algorithms. This decomposition provably preserves the optimal solution of the original HAD-MFC. Experiments show our method effectively identifies more vulnerable agents in large-scale MARL and the rule-based system, fooling system into worse failures, and learns a value function that reveals the vulnerability of each agent.

1 Introduction

Mean-field multi-agent reinforcement learning (MARL) [1, 2, 3, 4] has significantly enhanced the scalability of MARL through mean-field approximation, making it applicable to many large-scale real-world applications, such as robot swarm control [5, 6], voltage control [7], and traffic control [8]. However, given the large number of agents in such systems, it is likely that a small portion will deviate from the original policy during real-world deployment. For instance, in a thousand-robot swarm, individual robots may encounter action uncertainty [9] from software or hardware errors [10], environmental hazards [11], or even be controlled by adversaries [12, 13, 14, 15, 16]. As agent policies are interconnected in mean-field MARL, it is crucial to evaluate the impact of the failure of a small group of agents on the entire system.

In this paper, we focus on vulnerable agent identification (VAI) in large-scale MARL systems. This allows practitioners to enhance system robustness by providing these agents with targeted monitoring and protection. We further evaluate the system’s worst-case robustness under adversarial attacks [14], offering practitioners the worst-case performance of the system.

Critics may argue that vulnerable agents do not exist, as theoretical Mean-Field Controls assume all agents take identical actions [17, 3]. However, in real-world large-scale MARL systems, agents often have different initializations, local states, or interact with limited neighbors [6, 1], leading to agent variability. In such cases, a mean-field approximation remains relevant but does not assume full agent homogeneity. Research in network science has tackled *influence maximization* [18, 19, 20], which seeks to select a group of nodes in rule-based social networks to maximize their influence. However, these studies typically assume known graph structures, transition dynamics, and influence rules, which are absent in our setting. Identifying vulnerable agents has also been explored in small-scale MARL systems [21, 22, 23]. The primary challenge arises from scale: a 10-agent system has only $\binom{10}{1}$ possible scenarios, while a 1000-agent system yields $\binom{1000}{100}$ scenarios, an increase by a factor of 10^{139} . This represents a coupled problem where the upper level is a combinatorial problem, and the lower level involves mean-field MARL, making the complexity the central difficulty.

We begin by analyzing the complexity of the problem, which we formulate as a Hierarchical Adversarial Decentralized Mean Field Control (HAD-MFC). At the upper level, the task is to select M most vulnerable agents from a total of N , resulting in a combinatorial problem with complexity $\binom{N}{M}$. We show that this problem is NP-hard by reducing it to the generalized maximum coverage problem [24]. The lower level involves a mean-field MARL task, where an adversarial policy [14] is trained for the selected M vulnerable agents to assess the system’s worst-case robustness. Consequently, the overall challenge requires solving an NP-hard upper-level problem followed by a downstream mean-field MARL task.

To address the coupled problem of vulnerable agent identification, we first decouple the upper-level attacker with the lower-level one. Given a selected set of vulnerable agents at the upper level, we propose regularized mean-field Bellman operator that can evaluate the value function directly, under worst-case attack at lower level. The operator is derived by applying the Fenchel-Rockafellar transform [25, 26] to the uncertainty of vulnerable agents at the lower level. To solve the NP-hard upper-level problem, we formulate it as a MDP with dense rewards by the value function learned from our regularized mean-field Bellman operator, and solve it by greedy and RL algorithms. Next, we train a MARL policy on these selected vulnerable agents to evaluate the robustness of the large-scale MARL system. Finally, we prove that decomposing the original HAD-MFC into upper- and lower-level subproblems provably preserves the optimal solution of the original HAD-MFC. Experiments on large-scale MARL and rule-based systems show that our method outperforms baselines in 17 out of 18 tasks. It effectively identifies the most vulnerable agent, induces joint failures, and learns an interpretable value function that reveals agent vulnerabilities.

Contributions. Our contributions are twofold. First, we address the robustness of large-scale MARL by proposing the problem of vulnerable agent identification (VAI), formulating it as a HAD-MFC, and analyzing its hardness. Second, we show that HAD-MFC can be solved by decomposing the hierarchical process into two separate problems via Fenchel-Rockafellar transform and solve the upper-level NP-hard problem via formulating it as a MDP with dense reward.

2 Related Work

Learning Large-Scale MARL. In MARL, modeling the interactions between individual agents becomes impractical as the number of agents increases, making conventional MARL ineffective in large-scale [27]. Mean-Field Games (MFGs) [28, 17] offer a solution by modeling the overall distribution of agents, instead of individual agents. Recent advances in equilibrium learning for MFGs [29, 30, 4, 31, 32] have established strong theoretical foundations. Mean-Field Control (MFC) serves as the cooperative counterpart to MFGs [33, 34, 35]. Both frameworks assume a scenario where an infinite number of agents follow the same action distribution forming an mean field. However, in practical settings, agents need to take different actions based on their local states or specific policies. To address this, [1] extended the mean-field approximation to Markov games by modeling opponents through an action mean field using a Taylor expansion. This approach has been expanded to accommodate various MARL settings, including stationary [36], multi-type [37], and partially observable environments [38]. A more structured framework, known as decentralized MFGs [2], has also been developed, with significant contributions from [39, 40, 41]. Our study utilizes this decentralized framework, which has been proven to be highly effective in large-scale MARL [6].

Adversarial Attacks for MARL. The goal of adversarial attacks for MARL is to develop worst-case adversarial attacks of MARL under uncertainties. This includes uncertainties in state [15, 21, 22, 23], action [42, 43], or environment [44, 45] to cause a well-trained MARL algorithm to fail during testing. Among these studies, several focus on selecting the most vulnerable agents to attack. For instance, GMA-FGSM [22] groups agents by their features and selects vulnerable agents based on their contribution to the total reward. ARTS [46] evaluates system robustness by repeatedly selecting random groups of agents to act as attackers. The work most similar to ours is RTCA [23], which employs a differential evolution algorithm to select vulnerable agents. However, these approaches are confined to small-scale MARL, and the challenge of scaling them to large-scale MARL remains unexplored.

Influence Maximization. First proposed by [18], influence maximization involves selecting a set of nodes in a social network to influence the opinions of others through predefined rules. [18] demonstrated that this problem is NP-hard and introduced a greedy algorithm to solve it. Early works relied on heuristics, such as degree centrality [47, 48], graph structure [49, 50], genetic algorithms [51, 52], and community-based methods [53, 54]. More recent works address the problem by combining graph neural networks and reinforcement learning, learning a network embedding that serves as input to an RL algorithm for sequential node selection [55, 56, 57]. In contrast to these approaches, [58] demonstrated the potential to learn directly from network embeddings. However, most influence maximization studies assume a *known* graph, transition dynamics, and operate within a rule-based system. Our work does not rely on any of these assumptions.

3 Problem Formulation

3.1 Hierarchical Adversarial Decentralized Mean-Field Control

We formulate our problem as a Hierarchical Adversarial Mean-Field Control (HAD-MFC). To model large-scale MARL that assumes heterogeneous agents with mean-field approximations, we base our definition on decentralized Mean-Field Control (D-MFG) [2]. Next, HAD-MFC adapts D-MFG by fixing the victim policy and training an adversarial policy to (1) select a subset of agents from the victim agents (*i.e.*, agents not being attacked) and (2) replace the selected agents' policies with a worst-case adversarial policy. The HAD-MFC is defined as follows:

$$\mathcal{G} := \langle \mathcal{N}, \mathcal{S}, \mathcal{A}, \mathcal{P}, R, \mu_0, \nu_0, \gamma \rangle,$$

where $\mathcal{N} = \{1, \dots, N\}$ represents the set of N agents, \mathcal{S} and \mathcal{A} denote the finite state and action spaces for each agent. $\mathcal{P} : \mathcal{S} \times \mathcal{A} \times \Delta(\mathcal{S}) \times \Delta(\mathcal{A}) \rightarrow \Delta(\mathcal{S})$ is the state transition probability function, $R : \mathcal{S} \times \mathcal{A} \times \Delta(\mathcal{S}) \times \Delta(\mathcal{A}) \rightarrow \mathbb{R}$ is the shared reward function, $\mu_0 \in \Delta(\mathcal{S})$ and $\nu_0 \in \Delta(\mathcal{A})$ are the initial state and action distributions, and $\gamma \in [0, 1)$ is the discount factor. The interactions between agents are modeled through the mean-field state $\Delta(\mathcal{S})$ and action distribution $\Delta(\mathcal{A})$ in both the environment dynamics and rewards.

Let $\mathcal{T} = \{0, 1, \dots, T\}$ represent the set of time steps. At $t = 0$, the attacker selects k agents to form an attack set \mathcal{K} , where $\mathcal{K} \subseteq \mathcal{N}$ and $|\mathcal{K}| = k$, which remains fixed in the episode. At each time step $t \in \mathcal{T}$, each agent i receives a local state $s_t^i \in \mathcal{S}$ and estimates the empirical mean-field state $\mu_t(s) = \frac{1}{N} \sum_{j \in \mathcal{N}} \delta(s_t^j = s)$, with δ the Dirac's delta. Each agent first executes a fixed, well-trained cooperative policy $\pi_\beta(a_t^i | s_t^i, \mu_t) : \mathcal{S} \times \Delta(\mathcal{S}) \rightarrow \Delta(\mathcal{A})$. To model the policy deviation under uncertainty, we assign a perturbation budget $\epsilon^i \in [0, 1]$ for each agent. If agent i is in attack set \mathcal{K} , the adversary learns an adversarial action perturbation policy $\pi_\alpha(a_t^i | s_t^i, \mu_t) : \mathcal{S} \times \Delta(\mathcal{S}) \rightarrow \Delta(\mathcal{A})$, and yields a perturbed policy $\hat{\pi}^i = \epsilon^i \pi_\alpha^i + (1 - \epsilon^i) \pi_\beta^i \in \Delta(\mathcal{A})$, following the definition of PR-MDP in [9]. If agent i is not in attack set \mathcal{K} , the victim executes $\hat{\pi} = \pi_\beta$ with $\epsilon^i = 0$. The empirical mean-field action is $\nu_t(a) = \frac{1}{N} \sum_{j \in \mathcal{N}} \delta(a_t^j = a)$. The reward at time t is given by $r_t = R(s_t^i, a_t^i, \mu_t, \nu_t)$, which is shared across agents. The game then transitions to time $t + 1$, generating a new local state for each agent based on the environment transition $p(s_{t+1}^i | s_t^i, a_t^i, \mu_t, \nu_t)$. The expected reward is:

$$J(\hat{\pi}) \equiv J(\pi_\alpha, \pi_\beta) = \mathbb{E}_{\pi_\alpha, \pi_\beta} \left[\sum_{t=0}^{\infty} \gamma^t R(s_t^i, a_t^i, \mu_t, \nu_t) \right]. \quad (1)$$

Attacker's goal. The attacker's goal is to select an attack set \mathcal{K} such that the agents in \mathcal{K} learn an adversarial policy to minimize the expected reward:

$$\min_{\mathcal{K} \subseteq \mathcal{N}, |\mathcal{K}|=k} \min_{\pi_\alpha} J(\pi_\alpha, \pi_\beta). \quad (2)$$

Complexity issue. The attacker face a hierarchical problem. The upper level face a combinatorial problem to select the k most vulnerable agents, and the lower level learns an adversarial policy for these selected agents. The coupled nature characterize the complexity issue of our problem.

Relation to existing formulations. Our definition of HAD-MFC is distinct yet related to several existing formulations in the literature. Our study focus on control of practical large-scale MARL with mean-field approximation [2, 34] rather than theoretical MFGs and MFCs [29, 31, 33], and specifically focuses on the selection of vulnerable agents rather than equilibrium learning and optimal agent control. Our upper-level problem of selecting vulnerable agents is conceptually similar to influence maximization (IM) [18]. However, unlike IM, where influencing agents follow predefined rules, our framework requires agents to learn an adversarial policy and to cooperate optimally with other adversarial agents. Our lower-level problem is related to adversarial attacks in MARL [14]. Existing works either do not involve the selection of vulnerable agents [15, 43], or are limited to small-scale settings [21, 23]. Our approach addresses adversarial attacks in large-scale MARL environments using mean-field approximations, which are significantly more complex than previously studied methods.

3.2 Assumptions and Theoretical Analysis

In this section, we outline the assumptions underlying our attack model. Building on existing studies on adversarial MARL [9, 14, 59, 16], we introduce a practical threat model based on specific assumptions regarding the capabilities of both victims and attackers at different levels.

Assumption 3.1 (Victim’s capability). *Victims follow a fixed, well-trained policy π_β that remains unchanged during the attack.*

We assume that the victim policies are fixed to simulate an attack scenario at test time, where the large-scale MARL system is deployed and its policy does not adapt in response to the attack [9, 14]. We now describe the assumptions concerning the attackers.

Assumption 3.2 (Upper-level attacker’s capabilities and limitations). *The upper-level attacker can select k agents from \mathcal{N} and assign them perturbation budget $\epsilon_{i \in \mathcal{K}}^i = \epsilon$ only at the beginning of an episode. The upper-level attacker has access to all agents’ trajectories under the cooperative case, $\tau = [\{s_0^i\}_{i \in \mathcal{N}}, \{a_0^i\}_{i \in \mathcal{N}}, \mu_0, \nu_0, r_0, \dots, \{s_T^i\}_{i \in \mathcal{N}}, \{a_T^i\}_{i \in \mathcal{N}}, \mu_T, \nu_T, r_T]$. During the attack, it can also access the local state $\{s_t^i\}_{i \in \mathcal{N}}$ of all agents at $t = 0$ and the cumulative reward $r = \sum_{t \in \mathcal{T}} \gamma^t r_t$. It does not have access to the policy parameters of the victim agents.*

Proposition 3.3 (Hardness). The problem faced by the upper-level attacker is NP-hard.

Proof sketch. This is proven by reducing the problem to the generalized maximum coverage problem, which is NP-hard [24]. See full proof in Appendix. A.1. \square

Assumption 3.4 (Lower-level attacker’s capabilities and limitations). *The lower-level attacker $\min_{\pi_\alpha} J(\pi_\alpha, \pi_\beta)$ has access to its local state s_t^i , the empirical mean field μ_t, ν_t , and the reward r_t . It does not have access to the policies, value functions, or local states of other agents.*

Our upper-level attacker only requires access to cooperative trajectory data, which is relatively easy to obtain. Furthermore, our attack model is *black-box* for both upper-level and lower-level, without the need of victim’s policy (note that for lower-level attacker, its policy is added on, yet irrelevant to victim policy). Lastly, we establish the existence of an optimal adversary.

Proposition 3.5 (Existence of optimal adversary). For any HAD-MFC, there exists an optimal (i.e., most harmful) upper-level adversary \mathcal{K} and a corresponding lower-level adversary π_α .

Proof sketch. The upper-level attack is a finite combinatorial problem with an optimal solution. At the lower level, with fixed victim policies treated as part of the environment, the attacker solves a MFC problem with optimal solution. The optimal adversary exists by exploring all upper-level configurations and selecting the best lower-level policy. See full proof in Appendix. A.2. \square

4 Method

In this section, we propose algorithms to solve the complexity issue of HAD-MFC. We begin by decoupling the hierarchical problem, eliminating the need to train a worst-case lower-level adversary by reformulating it into a regularized mean-field Bellman operator. We then formulate the upper-level combinatorial task as a MDP with dense reward computed from the value function from the regularized mean-field Bellman operator, and solve it via greedy algorithm or RL.

4.1 Decoupling the Hierarchical Problem

Training the worst-case adversary π_α is computationally expensive since it requires solving the RL problem $\min_{\pi_\alpha} J(\pi_\alpha, \pi_\beta)$. To address this, we propose a regularized mean-field Bellman operator that efficiently estimates the value function under a worst-case adversary, using cooperative trajectories only. Our approach involves defining the Bellman function for the adversary, characterizing the uncertainty set induced by π_α , and applying Fenchel-Rockafellar transform to derive the solution.

Bellman operators. To begin, we define the value function $V^i(s^i, \mu)$ for our problem:

$$V^i(s^i, \mu) = \mathbb{E} \left[\sum_{t=0}^{\infty} \gamma^t r_t \mid s_0 = s, \mu_0 = \mu, a_t^i \sim \hat{\pi}(\cdot | s_t^i, \mu_t) \right]. \quad (3)$$

The Bellman operator $\mathcal{B}^{\hat{\pi}}$ with victim and adversary policy can be defined as:

$$(\mathcal{B}^{\hat{\pi}} V^i)(s^i, \mu) = \sum_{a \in \mathcal{A}} \hat{\pi}(a^i | s^i, \mu) \nu(a) \left[r + \gamma \sum_{s' \in \mathcal{S}} p(s'^i | s^i, a^i, \mu, \nu) V(s'^i, \mu') \right]. \quad (4)$$

With worst-case adversary, we can further define the worst-case Bellman operator as:

$$(\hat{\mathcal{B}}^{\hat{\pi}} V^i)(s^i, \mu) = \min_{\pi_\alpha} (\mathcal{B}^{\hat{\pi}} V^i)(s^i, \mu) \quad (5)$$

Uncertainty set characterization. We proceed by characterizing the impact of π_α on perturbed policy $\hat{\pi}$ and the perturbed mean-field action $\nu(a)$. We expand them as:

$$\begin{aligned} \hat{\pi}^i &= \epsilon^i \pi_\alpha^i + (1 - \epsilon^i) \pi_\beta^i, \quad \lim_{N \rightarrow \infty} \nu(a) = \xi \nu_\alpha(a) + (1 - \xi) \nu_\beta(a), \\ \text{where } \xi &= \frac{1}{N} \sum_{i \in \mathcal{N}} \epsilon^i, \nu_\alpha(a) = \frac{1}{N} \sum_{i \in \mathcal{N}} \delta(a_t^i = a | \pi_\alpha), \nu_\beta(a) = \frac{1}{N} \sum_{i \in \mathcal{N}} (1 - \epsilon^i) \delta(a_t^i = a | \pi_\beta). \end{aligned} \quad (6)$$

We can then derive the uncertainty set induced by π_α :

Proposition 4.1. The difference of perturbed policy and victim policy, as well as perturbed mean-field action and victim mean-field action can be (approximately) bounded in ℓ_p norm:

$$\|\hat{\pi}^i - \pi_\beta^i\|_p \leq 2^{1/p} \epsilon^i, p(\|\nu(a) - \nu_\beta(a)\|_p - 2^{1/p} \xi \geq \delta) \leq 2 \exp(-2N\delta^2), \forall \delta > 0. \quad (7)$$

Proof sketch. The proof for $\hat{\pi}$ is by expanding itself and $\|\pi_\alpha - \pi_\beta\|_p \leq 2^{1/p}$. The proof for ν is by Jensen's inequality and the probability is by Hoeffding's inequality. To avoid overly cluttered expressions, we drop the constant $2^{1/p}$ and simplify the expression as $\|\hat{\pi}^i - \pi_\beta^i\|_p \leq \epsilon^i$ and $\|\nu(a) - \nu_\beta(a)\| \lesssim \xi$ in subsequent derivations. See full proof in Appendix.A.3.

Fenchel-Rockafellar transform. With uncertainty set defined, we simplify the notation by $\hat{\pi}_\alpha^i = \hat{\pi}^i - \pi_\beta^i$ and $\hat{\nu}_\alpha(a) = \nu(a) - \nu_\beta(a)$, which is bounded by $\|\hat{\pi}_\alpha^i\|_p \leq \epsilon^i$ and $\hat{\nu}_\alpha(a) \lesssim \xi$ by Proposition. 4.1. We proceed by expanding the Bellman equation in Eqn. 5:

$$(\mathcal{B}^{\hat{\pi}} V^i)(s^i, \mu) = \sum_{a^i, a \in \mathcal{A}} (\hat{\pi}_\alpha^i + \pi_\beta^i) (\hat{\nu}_\alpha(a) + \nu_\beta(a)) \left[r_t + \gamma \sum_{s' \in \mathcal{S}} p(s' | s^i, a^i, \mu, \nu) V(s', \mu') \right]. \quad (8)$$

As we have proved in Proposition 3.5, an optimal adversary always exists. With $(\mathcal{B}^{\hat{\pi}} V^i)(s^i, \mu) = \min_{\pi_\alpha} (\mathcal{B}^{\hat{\pi}} V^i)(s^i, \mu)$, we then have the following robust feasible inequality [60]:

$$V^i(s^i, \mu) = (\mathcal{B}^{\hat{\pi}} V^i)(s^i, \mu) \leq (\hat{\mathcal{B}}^{\hat{\pi}} V^i)(s^i, \mu), \quad V^i(s^i, \mu) - (\hat{\mathcal{B}}^{\hat{\pi}} V^i)(s^i, \mu) \leq 0, \quad (9)$$

with equality holds when π_α reach optimality π_α^* . Thus, we are solving the following problem via Fenchel-Rockafellar transform [25, 26]:

$$\max_{\pi_\alpha} V^i(s^i, \mu) - (\hat{\mathcal{B}}^{\hat{\pi}} V^i)(s^i, \mu). \quad (10)$$

Proposition 4.2. The Fenchel-Rockafellar transform of Eqn. 10 results in a regularized mean-field Bellman operator $\mathcal{B}_{\epsilon^i, \xi}^R$:

$$\begin{aligned} \max_{\pi_\alpha} V^i(s^i, \mu) - (\hat{\mathcal{B}}^{\hat{\pi}} V^i)(s^i, \mu) &= V^i(s^i, \mu) - \mathcal{B}_{\epsilon^i, \xi}^R V^i(s^i, \mu, \epsilon^i, \xi) \\ &= V^i(s^i, \mu) - (\mathcal{B}^{\pi_\beta} V^i)(s^i, \mu) + (\epsilon^i + \xi + \epsilon^i \xi) \|Q^i(s^i, a^i, \mu, \nu)\|_q. \end{aligned} \quad (11)$$

Here, $1/p + 1/q = 1$ is the dual of ℓ_p norm via Fenchel-Rockafellar transform. In this way, our learned value function $V^i(s^i, \mu, \epsilon^i, \xi)$ estimated from our Bellman estimator $\mathcal{B}_{\epsilon^i, \xi}^R$ accounts for the value of agent i under attack, condition on current situation whether (1) ϵ^i , which indicates if agent i itself is perturbed, and (2) the mean-field approximation on ξ , the number of its teammates gets perturbed.

Proof sketch. We first expand $\hat{\pi}$ and $\nu(a)$ in Eqn. 5, resulting in a Q function with uncertainty. Applying Fenchel-Rockafellar transform completes the proof. See full proof in Appendix. A.4. \square

Proposition 4.3 (Contraction). The regularized mean-field Bellman operator $\mathcal{B}_{\epsilon^i, \xi}^R V^i(s^i, \mu, \epsilon^i, \xi) = (\mathcal{B}^{\pi_\beta} V^i)(s^i, \mu) + (\epsilon^i + \xi + \epsilon^i \xi) \|Q^i(s^i, a^i, \mu, \nu)\|_q$ is a contraction operator.

Proof sketch. To proof that, we find $\|Q^i(s^i, a^i, \mu, \nu)\|_q$ term cancels each other and the rest follows standard approach. See full proof in Appendix. A.5. \square

Proposition 4.4 (Relation to worst-case Q function). To understand our Bellman operator, we show $\epsilon^i \xi \|Q^i(s^i, a^i, \mu, \nu)\|_q$ is identical to the gap between the cooperative and worst-case Q function under ℓ_1 norm bounded perturbed action a_α^i and mean-field action ν_α induced by π_α :

$$\epsilon^i \xi \|Q^i(s^i, a^i, \mu, \nu)\|_q = \max_{\|a_\alpha^i\|_p \leq \epsilon^i, \|\nu_\alpha\|_p \leq \xi} \|Q^i(s^i, a^i, \mu, \nu) - Q^i(s^i, (a^i + a_\alpha^i), \mu, (\nu + \nu_\alpha))\|_1. \quad (12)$$

Proof sketch. The proof is done by first making a linear approximation of Q function, then applying Hölder’s inequality. See full proof in Appendix. A.6.

Remark 1. The regularization terms in \mathcal{B}^R arises from uncertainties in agents and the mean-field. To clarify, the term $\epsilon^i \|Q^i(s^i, a^i, \mu, \nu)\|_q$ capture agent vulnerability, $\xi \|Q^i(s^i, a^i, \mu, \nu)\|_q$ capture mean-field vulnerability, and $\epsilon^i \xi \|Q^i(s^i, a^i, \mu, \nu)\|_q$ capture vulnerability of their interactions. Each term yields more pessimistic value estimation when there are larger uncertainties in its actions, mean-field, or their interactions.

Remark 2. Notably, our approach does not assume π_β to be optimal, which means it can be extended to agent-based systems governed by predefined rules [61], provided these rules can be derived from Q-functions (*e.g.*, using a Boltzmann-based policy).

4.2 Algorithm for Vulnerable Agent Identification

In this section, we give a practical algorithm to solve upper-level vulnerable agent identification. We formulate this NP-hard problem as a MDP with dense reward calculated by regularized mean-field Bellman operator. We next propose RL and greedy algorithm for solving this MDP. Finally, we prove the decomposition of HAD-MFC do not alter the optimal solution.

Problem formulation. The problem faced by the upper-level adversary can be formulated as a Markov Decision Process, defined based on HAD-MFC:

$$\mathcal{M} := \langle \mathcal{S}, \epsilon, \mathcal{N}, \tilde{\mathcal{P}}, \tilde{R}, \gamma \rangle,$$

where $\mathcal{S} = \times_{i \in \mathcal{N}} \mathcal{S}^i$ is the local state space of each agent. The game proceeds in K steps, with K the number of adversaries we select. At step k , $\epsilon_k \in [0, 1]^N = \{\epsilon_k^i\}_{i \in \mathcal{N}}$ is the perturbation budget of each agent at step k , with $\epsilon_0^i = 0, \forall i \in \mathcal{N}$. \mathcal{N} is the action space, where agents could be selected as vulnerable agent, $\tilde{\mathcal{P}} : \mathcal{S} \times \mathcal{N} \rightarrow \mathcal{S}$ is the state transition, and $\tilde{R} : \mathcal{S} \times \mathcal{N} \times [0, 1] \rightarrow \mathbb{R}$ is the reward function, γ is the discount factor. At each step k , we select the most vulnerable agent n , and update the value of ϵ_k . Note that if we merge ϵ in \mathcal{S} , the problem becomes a standard MDP.

Reward. Reward specifies the objective of MDP. In our case, the reward is defined as: given the set of selected vulnerable agents \mathcal{K}_{k-1} and the new selected agent n_k at step k , what is the amount of reward the victim large-scale MARL system going to decrease, had it face the worst-case adversary trained on this new set of selected vulnerable agents $\mathcal{K}_k = \mathcal{K}_{k-1} \cup n_k$?

To calculate this value efficiently, we resort to the regularized mean-field Bellman operator $\mathcal{B}_{\epsilon^i, \xi}^R$ in Eqn. 4.2, which defines the amount of reward we expected to receive, given the ℓ_p bounded perturbation magnitude ϵ_k^i and ξ_k at step k . Define the value function learned under $\mathcal{B}_{\epsilon^i, \xi}^R$ at time $t = 0$ as $V^i(s_0^i, \mu_0, \epsilon_k^i, \xi_k)$, the reward can then be defined as:

$$r_k = \tilde{R}(s_k, \epsilon_k, n_k) = \frac{1}{N} \sum_{i \in \mathcal{N}} (V^i(s_0^i, \mu_0, \epsilon_k^i, \xi_k) - V^i(s_0^i, \mu_0, \epsilon_{k-1}^i, \xi_{k-1})). \quad (13)$$

Here ϵ_k^i can take any values between $[0, 2^{1/p}]$ and ξ_k depends on ϵ_k^i . We thus define the TD loss as:

$$\min \mathbb{E}_{\tau \sim \pi_\beta} (V^i(s^i, \mu, \epsilon^i, \xi) - r - \gamma V^i(s^i, \mu', \epsilon^i, \xi) + (\epsilon^i \xi + \epsilon^i + \xi) \|Q^i(s^i, a_\beta^i, \mu, \nu_\beta)\|_q)^2, \quad (14)$$

with $\epsilon \sim \text{Uniform}[0, 2^{1/p}]$, $\xi \sim \text{Bernouli}(\xi)$. This can be optimized using sampled trajectory in cooperative case (*i.e.*, $\tau \sim \pi_\beta$), which can be easy to obtain.

Solving the MDP. Given the RL formulation, we can optimize our VAI problem using any RL algorithm, such as Q-learning [62]. The Q function can be updated via standard TD loss. We call this approach as VAI-RL. Alternatively, the reward defined in Eqn. 13 suggests a fast greedy algorithm, such that the agent to maximize reward is selected at each step. We call this approach VAI-Greedy. We include both algorithms for comparison. See the pseudo code of both methods in Appendix. B.

Proposition 4.5 (Optimality of Decomposition). Given a HAD-MFC $\mathcal{G} := \langle \mathcal{N}, \mathcal{S}, \mathcal{A}, \mathcal{P}, R, \mu_0, \nu_0, \gamma \rangle$. For the upper-level MDP $\mathcal{M} := \langle \mathcal{S}, \epsilon, \mathcal{N}, \hat{\mathcal{P}}, \hat{R}, \gamma \rangle$ with reward defined in Eqn. 13, and the value $V^{i,*}(s^i, \mu, \epsilon^i, \xi)$ of lower-level problem is learned by regularized mean-field Bellman operator $\mathcal{B}_{\epsilon^i, \xi}^R$, define the optimal vulnerable agents of \mathcal{M} as $\mathcal{K}^* \subseteq \mathcal{N}$. The selected vulnerable agents $\mathcal{K}^* \subseteq \mathcal{N}$ and the worst-case adversarial policy learned π_α^* under $\mathcal{K}^* \subseteq \mathcal{N}$ is the optimal solution of HAD-MFC.

Proof sketch. The optimality of lower-level policy π_α^* is done by the property of Rockfellar-Fenchel transform. The optimality of higher-level problem follows the fact that optimal solution exists in MDP. See full proof in Appendix. A.7.

5 Experiments

Environments. We evaluate our algorithms in three environments: Battle [6], Taxi Matching [8], and Vicsek [63]. The Vicsek environment is used to test our algorithm in rule-based systems. Detailed descriptions of the environments are provided in Appendix C.1. We train all victim agents in Battle using MF-Q, and Taxi Matching using MF-AC [1], which empirically yields better task performance.

Baselines. To our knowledge, the problem of vulnerable agent identification in MARL is rarely studied in literature. Therefore, we select five relevant studies as baselines: (1) Random selection, serving as a simple baseline. (2) Degree centrality (DC) [64], a heuristic method that select agents with the most connections with others. (3) Bi-level RL [65], which trains our upper-level and lower-level problems hierarchically. (4) PIANO [56], which selects critical agents iteratively via graph embeddings and RL. (5) RTCA [23], which selects vulnerable agents in small-scale MARL using differential evolution. For methods requiring a graph structure, we construct an undirected graph with an edge of weight 1 between two agents if they can observe each other, and 0 otherwise. We call our method as Vulnerable Agent Identification (VAI). All baselines are trained using the same codebase, network structure, and hyperparameters to ensure fair comparison. Detailed implementations and hyperparameters are provided in Appendices C.2 and C.3.

Evaluation protocol. We consider $\{\epsilon^i\}_{i \in \mathcal{K}} = 1$ bounded by ℓ_∞ norm. The setting allows adversaries to manipulate the policy of π_β arbitrarily. The scenario occurs when agents crash in the environment, or are compromised by the adversary [10, 11, 14]. Results of different ϵ in Appendix. D.2. The number of attackers, K , is empirically determined based on the total number of agents in the environment. We report the results on victims and attackers with five random seeds.

5.1 Simulation Results

Table 1: Performance of our VAI-RL and VAI-Greedy in three environments, each with two map sizes and different numbers of attackers. Our VAI methods consistently achieve better attack capability.

Environment: Battle (↓)								
Agent Num	Adv. Num	Random	DC	Bi-Level RL	PIANO	RTCA	VAI-Greedy	VAI-RL
64	8	298.47±76.56	305.16±45.39	295.09±12.96	296.79±47.67	301.08±22.72	287.53±9.39	281.50±17.33
	16	97.33±34.52	93.54±34.56	87.37±6.28	81.06±11.34	85.71±24.62	72.01±20.28	77.73±1.81
	32	-152.89±26.75	-160.51±75.32	-198.03±55.83	-175.24±39.11	-192.78±43.81	-214.40±43.12	-929.88±62.73
144	18	730.65±117.42	693.15±98.87	685.77±124.51	670.55±66.75	650.33±50.47	610.62±31.36	505.34±30.79
	36	250.43±120.19	140.67±76.67	189.95±15.54	130.63±34.69	155.02±170.74	85.52±35.11	86.26±38.72
	72	-1809.01±130.98	-2014.57±670.92	-2353.78±870.53	-2313.46±230.66	-2221.12±360.49	-2579.80±256.19	-2837.83±482.56
Environment: Taxi (↓)								
Agent Num	Adv. Num	Random	DC	Bi-Level RL	PIANO	RTCA	VAI-Greedy	VAI-RL
50	4	33.9±14.39	19.07±5.77	27.52±16.12	23.55±7.44	16.26±3.32	10.47±4.85	12.47±8.73
	16	109.94±7.32	79.01±11.33	162.23±2.31	140.60±49.01	138.73±1.72	54.63±8.81	64.72±3.76
	36	617.09±51.80	595.80±60.28	571.26±59.96	516.91±44.86	618.21±54.08	463.70±55.99	365.96±63.75
100	4	34.49±22.61	21.17±3.47	14.17±3.07	36.51±6.11	16.87±8.27	8.27±8.67	4.95±2.86
	16	172.00±75.41	141.19±5.80	201.14±68.66	202.51±47.18	140.76±32.44	153.97±8.52	186.62±40.79
	36	884.49±68.87	867.62±23.46	892.51±66.15	793.71±12.86	860.58±106.61	770.14±29.74	652.10±23.23
Environment: Vicsek (↑)								
Agent Num	Adv. Num	Random	DC	Bi-Level RL	PIANO	RTCA	VAI-Greedy	VAI-RL
100	20	-226.96±11.54	-232.45±3.77	-221.26±14.06	-250.83±19.59	-225.12±28.05	-167.60±3.91	-183.68±19.56
	35	-159.83±40.85	-143.14±42.37	-141.51±43.28	-162.74±28.45	-129.24±13.30	-113.64±15.78	-93.65±28.65
	50	-96.83±7.26	-95.22±6.19	-96.80±0.76	-86.21±3.55	-82.63±5.70	-70.52±5.21	-75.82±2.57
400	80	-884.34±53.96	-840.87±33.67	-780.31±90.02	-950.13±110.36	-872.21±130.11	-710.56±56.32	-659.65±86.73
	140	-480.17±50.16	-440.63±80.67	-460.43±74.71	-510.24±62.11	-410.14±87.33	-390.74±42.16	-302.76±76.37
	200	-295.13±36.94	-313.55±49.43	-310.78±56.89	-290.53±27.89	-287.53±46.76	-256.44±21.34	-275.62±37.76

First, we evaluate the effectiveness of our method on finding the most vulnerable agents to attack. This is done by (1) solve the upper-level problem of finding the most vulnerable agents and (2) solve the lower-level problem of learning a worst-case policy for these vulnerable agents. For comprehensiveness, for each task, we evaluate them on six subtasks, including two map sizes with different agent numbers in the game, and each map sizes with three different number of adversaries.

As shown in Table. 1, our VAI based method outperforms all baselines in 17 out of 18 tasks, while heuristic-based method and learning based method are only slightly better than random selection. To explain this, heuristic-based method such as degree centrality (DC) are designed for rule-based systems. However, in large-scale MARL, the interaction between agents are nonlinear and are not clearly defined by rules. For example, in Battle environment, agents in the center of the crowd are less susceptible to attack than the agents in frontline, combating enemies, making DC ineffective. As for learning-based method, PIANO do not account for the worst-case policy made by agents, thus are unable to select the set of most harmful agents under adversarial policies. Solving our problem via bi-level RL and RTCA do not work well due to the hierarchical nature of our problem, which may be too hard for RL to solve without any guidance. In contrast, our VAI method works well due to the more accurate value function we learned via Bellman operator $\mathcal{B}_{\epsilon^i, \xi}^R$.

Additionally, we observed that VAI-RL outperforms VAI-Greedy in 10 of 18 tasks, especially when more attackers are available. To explain, Greedy algorithm focuses on immediate reward and works well with less attackers and weak agent-wise interactions. RL, in contrast, models long-term returns and inter-agent impact, which performs better with more attackers. Additionally, RL provides theoretical guarantees for optimality in MDPs, which greedy methods lack.

Finally, we would like to highlight that our VAI algorithm yields superior results not only on MARL environments, but also on rule-based Vicsek environment. This is done by approximating a value function using collected rule-based trajectories, then estimate the vulnerability of each agent via our proposed Bellman operator $\mathcal{B}_{\epsilon^i, \xi}^R$. In this end, we expect our work to have future impacts in rule-based complex systems with real-world impact, such as social networks [18, 19].

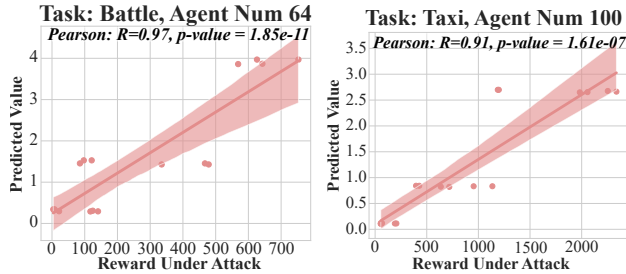


Figure 1: Pearson correlation between the lower-level attack value estimated by our Bellman operator $\mathcal{B}_{\epsilon^i, \xi}^R$ and lower-level reward by running an attack using RL.

Computational Efficiency: While our VAI requires training an additional function in Proposition 4.2, the overall computation cost is on par with our baselines. See full results in Appendix. D.1.

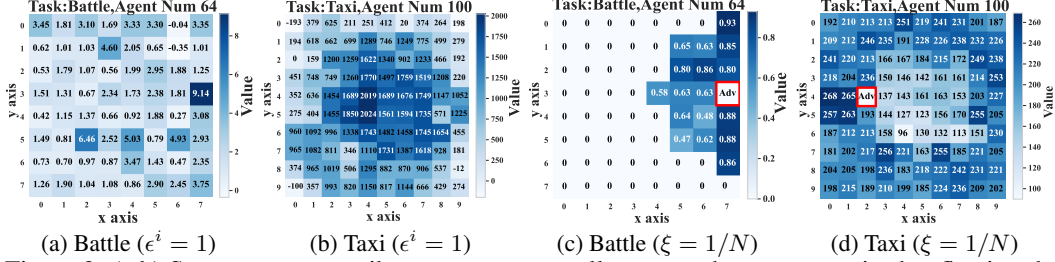
Results with Different ϵ : Under different perturbation budget ϵ , our VAI-RL and VAI-Greedy consistently outperform other baselines. See full results in Appendix. D.2.

5.2 Discussions and Insights

In this section, we thoroughly evaluate the effectiveness of our method, showing our theory is effective in practice and our method offers meaningful insights to the robustness of large-scale MARL.

Our Method is Effective by Value Estimation. We attribute the effectiveness of our methods via the regularized mean-field Bellman operator $\mathcal{B}_{\epsilon^i, \xi}^R$ in Proposition. 4.2. To verify this, we compare the results predicted by our value function of the lower-level attack, and the reward gained by actually running the lower-level attack via RL. As shown in Fig. 1, we find the value function learned by $\mathcal{B}_{\epsilon^i, \xi}^R$ is effective at predicting the attack result of the worst-case adversarial policy for vulnerable agent selections, showing strong Pearson correlation ($r = 0.97$ for Battle, $r = 0.91$ for Taxi, $p < .001$). Thus, $\mathcal{B}_{\epsilon^i, \xi}^R$ effectively decompose HAD-MFC by acting as a predictor of lower-level attack.

Certain agents are more vulnerable than others. In large-scale MARL systems, some agents play disproportionately critical roles, making them inherently more vulnerable. To illustrate this, we visualize agent values in the Battle-64 and Taxi-100 environments using heatmaps in Fig. 2, where each cell represents the importance of a single agent at the start of the game. In Battle-64, 64 agents are arranged in an 8×8 grid to engage with another team of 64 agents; we display only the 64 agents



(a) Battle ($\epsilon^i = 1$) (b) Taxi ($\epsilon^i = 1$) (c) Battle ($\xi = 1/N$) (d) Taxi ($\xi = 1/N$)
Figure 2: (a,b) Some agents contribute more to overall system when compromised, reflecting the change from $\epsilon^i = 0$ to $\epsilon^i = 1$. (c,d) Agents receive more impact when facing attackers, reflecting the change from $\xi = 0$ to $\xi = 1/N$. Darker cell indicates agents are more vulnerable under attacks.

controlled by the mean-field MARL policy. In Taxi-100, 100 agents are uniformly positioned across a 10×10 map. The heatmaps reveal two key factors on vulnerability:

First, some agents contribute more significantly to overall system functionality. Figs. 2a and 2b visualize the value difference $V^i(s^i, \mu, \epsilon^i = 0, \xi = 0) - V^i(s^i, \mu, \epsilon^i = 1, \xi = 0)$, reflecting the drop in value if agent i is selected as an adversary, as captured by the ϵ^i term in Proposition 4.2. In Battle, agents at the right hand side engage enemies more frequently and thus accumulate more rewards, making them both more valuable and more vulnerable when compromised. In Taxi, ride requests occur more frequently near the center, so agents located there earn higher rewards and are similarly more critical. These patterns indicate that agents with advantageous positions or key roles contribute more to cooperation and are therefore prime targets for adversarial exploitation.

Second, the failure of one agent can negatively affect others. Figs. 2c and 2d show the impact of a single adversary (highlighted in a red square) on its teammates' value functions, computed as $V^i(s^i, \mu, \epsilon^i = 0, \xi = 0) - V^i(s^i, \mu, \epsilon^i = 0, \xi = 1/N)$, corresponding to the ξ term in Proposition 4.2. In Battle, disruption primarily affects agents in the same row, where coordination is essential for collective attacks. In Taxi, agents to the left suffer most, as they must move toward the central region, but are blocked by the adversary. In contrast, central agents remain largely unaffected. These results demonstrate that the learned V^i function captures inter-agent dependencies and accurately reflects vulnerability propagation within the team.

6 Conclusions

In this paper, we evaluate the extent to which the failure of a group of agents adopting worst-case policies impacts the robustness of large-scale MARL. We define this problem as Vulnerable Agent Identification (VAI) and formulate it as a HAD-MFC. In this hierarchical framework, the upper level addresses the NP-hard problem of selecting the most vulnerable agents, while the lower level learns worst-case adversarial policies. We disentangle this hierarchical problem using Fenchel-Rockafellar transform and solve the NP-hard upper-level problem with greedy algorithm and RL. Experiments show that our method identifies groups of vulnerable agents in both large-scale MARL and rule-based systems, causing these systems to experience joint failures, and learns a value function that accurately predicts the vulnerability of each agent. Future work will focus on extending our method to real-world systems with graph structures, such as social networks. While misuse is theoretically possible, it is mitigated by the method's greater utility to defenders and its reliance on trajectory data.

References

- [1] Yaodong Yang, Rui Luo, Minne Li, Ming Zhou, Weinan Zhang, and Jun Wang. Mean field multi-agent reinforcement learning. In *International conference on machine learning*, pages 5571–5580. PMLR, 2018.
- [2] Sriram Ganapathi Subramanian, Matthew E Taylor, Mark Crowley, and Pascal Poupart. Decentralized mean field games. In *Proceedings of the AAAI Conference on Artificial Intelligence*, volume 36, pages 9439–9447, 2022.
- [3] Barna Pasztor, Ilija Bogunovic, and Andreas Krause. Efficient model-based multi-agent mean-field reinforcement learning. *arXiv preprint arXiv:2107.04050*, 2021.

- [4] Mathieu Laurière, Sarah Perrin, Sertan Girgin, Paul Muller, Ayush Jain, Theophile Cabannes, Georgios Piliouras, Julien Pérolat, Romuald Elie, Olivier Pietquin, et al. Scalable deep reinforcement learning algorithms for mean field games. In *International Conference on Machine Learning*, pages 12078–12095. PMLR, 2022.
- [5] Maximilian Hüttenrauch, Sosc Adrian, Gerhard Neumann, et al. Deep reinforcement learning for swarm systems. *Journal of Machine Learning Research*, 20(54):1–31, 2019.
- [6] Lianmin Zheng, Jiacheng Yang, Han Cai, Ming Zhou, Weinan Zhang, Jun Wang, and Yong Yu. Magent: A many-agent reinforcement learning platform for artificial collective intelligence. In *Thirty-Second AAAI Conference on Artificial Intelligence*, 2018.
- [7] Jianhong Wang, Wangkun Xu, Yunjie Gu, Wenbin Song, and Tim C Green. Multi-agent reinforcement learning for active voltage control on power distribution networks. *Advances in Neural Information Processing Systems*, 34:3271–3284, 2021.
- [8] Duc Thien Nguyen, Akshat Kumar, and Hoong Chuin Lau. Credit assignment for collective multiagent rl with global rewards. *Advances in neural information processing systems*, 31, 2018.
- [9] Chen Tessler, Yonathan Efroni, and Shie Mannor. Action robust reinforcement learning and applications in continuous control. In *International Conference on Machine Learning*, pages 6215–6224. PMLR, 2019.
- [10] Eliahu Khalastchi and Meir Kalech. Fault detection and diagnosis in multi-robot systems: A survey. *Sensors*, 19(18):4019, 2019.
- [11] Xinge Huang, Farshad Arvin, Craig West, Simon Watson, and Barry Lennox. Exploration in extreme environments with swarm robotic system. In *2019 IEEE international conference on mechatronics (ICM)*, volume 1, pages 193–198. IEEE, 2019.
- [12] Sait Murat Giray. Anatomy of unmanned aerial vehicle hijacking with signal spoofing. In *2013 6th International Conference on Recent Advances in Space Technologies (RAST)*, pages 795–800. IEEE, 2013.
- [13] Bora Ly and Romny Ly. Cybersecurity in unmanned aerial vehicles (uavs). *Journal of Cyber Security Technology*, 5(2):120–137, 2021.
- [14] Adam Gleave, Michael Dennis, Cody Wild, Neel Kant, Sergey Levine, and Stuart Russell. Adversarial policies: Attacking deep reinforcement learning. *arXiv preprint arXiv:1905.10615*, 2019.
- [15] Jieyu Lin, Kristina Dzevaroska, Sai Qian Zhang, Alberto Leon-Garcia, and Nicolas Papernot. On the robustness of cooperative multi-agent reinforcement learning. In *2020 IEEE Security and Privacy Workshops (SPW)*, pages 62–68. IEEE, 2020.
- [16] Le Cong Dinh, David Henry Mguni, Long Tran-Thanh, Jun Wang, and Yaodong Yang. Online markov decision processes with non-oblivious strategic adversary. *Autonomous Agents and Multi-Agent Systems*, 37(1):15, 2023.
- [17] Jean-Michel Lasry and Pierre-Louis Lions. Mean field games. *Japanese journal of mathematics*, 2(1):229–260, 2007.
- [18] David Kempe, Jon Kleinberg, and Éva Tardos. Maximizing the spread of influence through a social network. In *Proceedings of the ninth ACM SIGKDD international conference on Knowledge discovery and data mining*, pages 137–146, 2003.
- [19] Suman Banerjee, Mamata Jenamani, and Dilip Kumar Pratihar. A survey on influence maximization in a social network. *Knowledge and Information Systems*, 62:3417–3455, 2020.
- [20] Yandi Li, Haobo Gao, Yunxuan Gao, Jianxiong Guo, and Weili Wu. A survey on influence maximization: From an ml-based combinatorial optimization. *ACM Transactions on Knowledge Discovery from Data*, 17(9):1–50, 2023.

- [21] Nhan H Pham, Lam M Nguyen, Jie Chen, Hoang Thanh Lam, Subhro Das, and Tsui-Wei Weng. Evaluating robustness of cooperative marl: A model-based approach. *arXiv preprint arXiv:2202.03558*, 2022.
- [22] Lixia Zan, Xiangbin Zhu, and Zhao-Long Hu. Adversarial attacks on cooperative multi-agent deep reinforcement learning: a dynamic group-based adversarial example transferability method. *Complex & Intelligent Systems*, 9(6):7439–7450, 2023.
- [23] Ziyuan Zhou and Guanjun Liu. Robustness testing for multi-agent reinforcement learning: State perturbations on critical agents. *arXiv preprint arXiv:2306.06136*, 2023.
- [24] Reuven Cohen and Liran Katzir. The generalized maximum coverage problem. *Information Processing Letters*, 108(1):15–22, 2008.
- [25] Ralph Tyrell Rockafellar. *Convex analysis*, 1970.
- [26] Ofir Nachum and Bo Dai. Reinforcement learning via fenchel-rockafellar duality. *arXiv preprint arXiv:2001.01866*, 2020.
- [27] Yaodong Yang and Jun Wang. An overview of multi-agent reinforcement learning from game theoretical perspective. *arXiv preprint arXiv:2011.00583*, 2020.
- [28] Minyi Huang, Roland P Malhamé, and Peter E Caines. Large population stochastic dynamic games: closed-loop mckean-vlasov systems and the nash certainty equivalence principle. *COMMUNICATIONS IN INFORMATION AND SYSTEMS*, 2006.
- [29] Xin Guo, Anran Hu, Renyuan Xu, and Junzi Zhang. Learning mean-field games. *Advances in neural information processing systems*, 32, 2019.
- [30] Julien Perolat, Sarah Perrin, Romuald Elie, Mathieu Laurière, Georgios Piliouras, Matthieu Geist, Karl Tuyls, and Olivier Pietquin. Scaling up mean field games with online mirror descent. *arXiv preprint arXiv:2103.00623*, 2021.
- [31] Paul Muller, Romuald Elie, Mark Rowland, Mathieu Lauriere, Julien Perolat, Sarah Perrin, Matthieu Geist, Georgios Piliouras, Olivier Pietquin, and Karl Tuyls. Learning correlated equilibria in mean-field games. *arXiv preprint arXiv:2208.10138*, 2022.
- [32] René Carmona, Mathieu Laurière, and Zongjun Tan. Model-free mean-field reinforcement learning: mean-field mdp and mean-field q-learning. *The Annals of Applied Probability*, 33(6B):5334–5381, 2023.
- [33] Haotian Gu, Xin Guo, Xiaoli Wei, and Renyuan Xu. Mean-field controls with q-learning for cooperative marl: convergence and complexity analysis. *SIAM Journal on Mathematics of Data Science*, 3(4):1168–1196, 2021.
- [34] Washim Uddin Mondal, Mridul Agarwal, Vaneet Aggarwal, and Satish V Ukkusuri. On the approximation of cooperative heterogeneous multi-agent reinforcement learning (marl) using mean field control (mfc). *Journal of Machine Learning Research*, 23(129):1–46, 2022.
- [35] Andrea Angiuli, Jean-Pierre Fouque, and Mathieu Laurière. Unified reinforcement q-learning for mean field game and control problems. *Mathematics of Control, Signals, and Systems*, 34(2):217–271, 2022.
- [36] Jayakumar Subramanian and Aditya Mahajan. Reinforcement learning in stationary mean-field games. In *Proceedings of the 18th International Conference on Autonomous Agents and MultiAgent Systems*, pages 251–259, 2019.
- [37] Sriram Ganapathi Subramanian, Pascal Poupart, Matthew E Taylor, and Nidhi Hegde. Multi type mean field reinforcement learning. *arXiv preprint arXiv:2002.02513*, 2020.
- [38] Sriram Ganapathi Subramanian, Matthew E Taylor, Mark Crowley, and Pascal Poupart. Partially observable mean field reinforcement learning. *arXiv preprint arXiv:2012.15791*, 2020.

- [39] Pier Giuseppe Sessa, Maryam Kamgarpour, and Andreas Krause. Efficient model-based multi-agent reinforcement learning via optimistic equilibrium computation. In *International Conference on Machine Learning*, pages 19580–19597. PMLR, 2022.
- [40] Kai Cui, Sascha Hauck, Christian Fabian, and Heinz Koepl. Learning decentralized partially observable mean field control for artificial collective behavior. *arXiv preprint arXiv:2307.06175*, 2023.
- [41] Kai Cui, Christian Fabian, Anam Tahir, and Heinz Koepl. Major-minor mean field multi-agent reinforcement learning. In *Forty-first International Conference on Machine Learning*, 2024.
- [42] Jun Guo, Yonghong Chen, Yihang Hao, Zixin Yin, Yin Yu, and Simin Li. Towards comprehensive testing on the robustness of cooperative multi-agent reinforcement learning. In *Proceedings of the IEEE/CVF conference on computer vision and pattern recognition*, pages 115–122, 2022.
- [43] Simin Li, Jun Guo, Jingqiao Xiu, Pu Feng, Xin Yu, Aishan Liu, Wenjun Wu, and Xianglong Liu. Attacking cooperative multi-agent reinforcement learning by adversarial minority influence. *arXiv preprint arXiv:2302.03322*, 2023.
- [44] Kaiqing Zhang, Tao Sun, Yunzhe Tao, Sahika Genc, Sunil Mallya, and Tamer Basar. Robust multi-agent reinforcement learning with model uncertainty. *Advances in neural information processing systems*, 33:10571–10583, 2020.
- [45] Laixi Shi, Eric Mazumdar, Yuejie Chi, and Adam Wierman. Sample-efficient robust multi-agent reinforcement learning in the face of environmental uncertainty. *arXiv preprint arXiv:2404.18909*, 2024.
- [46] Thomy Phan, Thomas Gabor, Andreas Sedlmeier, Fabian Ritz, Bernhard Kempter, Cornel Klein, Horst Sauer, Reiner Schmid, Jan Wieghardt, Marc Zeller, et al. Learning and testing resilience in cooperative multi-agent systems. In *Proceedings of the 19th International Conference on Autonomous Agents and MultiAgent Systems*, pages 1055–1063, 2020.
- [47] Wei Chen, Yajun Wang, and Siyu Yang. Efficient influence maximization in social networks. In *Proceedings of the 15th ACM SIGKDD international conference on Knowledge discovery and data mining*, pages 199–208, 2009.
- [48] Christo Wilson, Bryce Boe, Alessandra Sala, Krishna PN Puttaswamy, and Ben Y Zhao. User interactions in social networks and their implications. In *Proceedings of the 4th ACM European conference on Computer systems*, pages 205–218, 2009.
- [49] Wei Chen, Yifei Yuan, and Li Zhang. Scalable influence maximization in social networks under the linear threshold model. In *2010 IEEE international conference on data mining*, pages 88–97. IEEE, 2010.
- [50] Gennaro Cordasco, Luisa Gargano, Marco Mecchia, Adele A Rescigno, and Ugo Vaccaro. A fast and effective heuristic for discovering small target sets in social networks. In *Combinatorial Optimization and Applications: 9th International Conference, COCOA 2015, Houston, TX, USA, December 18-20, 2015, Proceedings*, pages 193–208. Springer, 2015.
- [51] Chun-Wei Tsai, Yo-Chung Yang, and Ming-Chao Chiang. A genetic newgreedy algorithm for influence maximization in social network. In *2015 IEEE International Conference on Systems, Man, and Cybernetics*, pages 2549–2554. IEEE, 2015.
- [52] Doina Bucur and Giovanni Iacca. Influence maximization in social networks with genetic algorithms. In *Applications of Evolutionary Computation: 19th European Conference, EvoApplications 2016, Porto, Portugal, March 30–April 1, 2016, Proceedings, Part I 19*, pages 379–392. Springer, 2016.
- [53] Yu Wang, Gao Cong, Guojie Song, and Kunqing Xie. Community-based greedy algorithm for mining top-k influential nodes in mobile social networks. In *Proceedings of the 16th ACM SIGKDD international conference on Knowledge discovery and data mining*, pages 1039–1048, 2010.

- [54] Yi-Cheng Chen, Wen-Yuan Zhu, Wen-Chih Peng, Wang-Chien Lee, and Suh-Yin Lee. Cim: Community-based influence maximization in social networks. *ACM Transactions on Intelligent Systems and Technology (TIST)*, 5(2):1–31, 2014.
- [55] Eli Meir, Haggai Maron, Shie Mannor, and Gal Chechik. Controlling graph dynamics with reinforcement learning and graph neural networks. In *International Conference on Machine Learning*, pages 7565–7577. PMLR, 2021.
- [56] Hui Li, Mengting Xu, Sourav S Bhowmick, Joty Shafiq Rayhan, Changsheng Sun, and Jiangtao Cui. Piano: Influence maximization meets deep reinforcement learning. *IEEE Transactions on Computational Social Systems*, 10(3):1288–1300, 2022.
- [57] Tiantian Chen, Siwen Yan, Jianxiong Guo, and Weili Wu. Touplegdd: A fine-designed solution of influence maximization by deep reinforcement learning. *IEEE Transactions on Computational Social Systems*, 11(2):2210–2221, 2023.
- [58] Chen Ling, Junji Jiang, Junxiang Wang, My T Thai, Renhao Xue, James Song, Meikang Qiu, and Liang Zhao. Deep graph representation learning and optimization for influence maximization. In *International Conference on Machine Learning*, pages 21350–21361. PMLR, 2023.
- [59] Simin Li, Jun Guo, Jingqiao Xiu, Ruixiao Xu, Xin Yu, Jiakai Wang, Aishan Liu, Yaodong Yang, and Xianglong Liu. Byzantine robust cooperative multi-agent reinforcement learning as a bayesian game. *arXiv preprint arXiv:2305.12872*, 2023.
- [60] Garud N Iyengar. Robust dynamic programming. *Mathematics of Operations Research*, 30(2):257–280, 2005.
- [61] Li An, Volker Grimm, Abigail Sullivan, BL Turner Ii, Nicolas Malleon, Alison Heppenstall, Christian Vincenot, Derek Robinson, Xinyue Ye, Jianguo Liu, et al. Challenges, tasks, and opportunities in modeling agent-based complex systems. *Ecological Modelling*, 457:109685, 2021.
- [62] Volodymyr Mnih, Koray Kavukcuoglu, David Silver, Andrei A Rusu, Joel Veness, Marc G Bellemare, Alex Graves, Martin Riedmiller, Andreas K Fidjeland, Georg Ostrovski, et al. Human-level control through deep reinforcement learning. *nature*, 518(7540):529–533, 2015.
- [63] Tamás Vicsek, András Czirók, Eshel Ben-Jacob, Inon Cohen, and Ofer Shochet. Novel type of phase transition in a system of self-driven particles. *Physical review letters*, 75(6):1226, 1995.
- [64] Marcel Salathé and James H Jones. Dynamics and control of diseases in networks with community structure. *PLoS computational biology*, 6(4):e1000736, 2010.
- [65] Alexander Sasha Vezhnevets, Simon Osindero, Tom Schaul, Nicolas Heess, Max Jaderberg, David Silver, and Koray Kavukcuoglu. Feudal networks for hierarchical reinforcement learning. In *International conference on machine learning*, pages 3540–3549. PMLR, 2017.
- [66] René Carmona, François Delarue, et al. *Probabilistic theory of mean field games with applications I-II*. Springer, 2018.
- [67] Richard Bellman. Dynamic programming. *science*, 153(3731):34–37, 1966.
- [68] Volodymyr Mnih, Koray Kavukcuoglu, David Silver, Andrei A Rusu, Joel Veness, Marc G Bellemare, Alex Graves, Martin Riedmiller, Andreas K Fidjeland, Georg Ostrovski, et al. Human-level control through deep reinforcement learning. *nature*, 518(7540):529–533, 2015.
- [69] Gabriel Dulac-Arnold, Richard Evans, Hado van Hasselt, Peter Sunehag, Timothy Lillicrap, Jonathan Hunt, Timothy Mann, Theophane Weber, Thomas Degris, and Ben Coppin. Deep reinforcement learning in large discrete action spaces. *arXiv preprint arXiv:1512.07679*, 2015.

APPENDIX FOR "VULNERABLE AGENT IDENTIFICATION IN LARGE-SCALE MULTI-AGENT REINFORCEMENT LEARNING"

A Proofs and Derivations

A.1 Proof of Proposition 3.3

To demonstrate the NP-hardness of our upper-level problem, we reduce it to the generalized maximum coverage problem [24].

Consider an instance of the generalized maximum coverage problem defined by [24] as follows: let $\mathbb{E} = \{e_1, \dots, e_n\}$ be a set of n elements, and let $\mathbb{B} = \{b_1, \dots, b_m\}$ be a collection of m bins. For each bin b and element e , there is a positive profit $P(b, e)$ and a non-negative weight $W(b, e)$. Each bin has a weight $W(b)$ as the overhead. The objective is to find a selection $f : \mathbb{E} \rightarrow \mathbb{B}$ that maps each element to a bin. The overall weight of this selection is $W(f) = \sum_{e \in \mathcal{E}} W(b, e) + \sum_{b \in \mathcal{B}} W(b)$, the profit of this selection is $P(f) = \sum_{e \in \mathcal{E}} P(b, e)$. The objective is to maximize $P(f)$, while satisfying the constraint $W(f) \leq C$, where C is a constant.

We can map our upper-level problem to this instance of the generalized maximum coverage problem by making the following correspondences. First, each agent in our problem corresponds to an element in the generalized maximum coverage problem. Second, the bin corresponds to if an agent is selected as an attacker or not, *i.e.*, a mapping $f : \mathcal{N} \rightarrow \mathcal{K}$. Third, the cumulative reward is defined as the overall weight of the mapping f : $r = P(f) = \sum_{e \in \mathcal{E}} P(b, e)$. Finally, the constraint is defined as the weight of each bin and element. In our setting, $W(b) = 0, \forall b \in \mathcal{B}$, $W(b, e) = 1$ if $e \in \mathcal{K}$ and $W(b, e) = 0$ otherwise. The constraint is defined by $W(f) = \sum_{e \in \mathcal{E}} W(b, e) + \sum_{b \in \mathcal{B}} W(b)$, with $W(f) \leq K$, where K is the number of adversaries. This establishes that our upper-level problem is a specific instance of the maximum coverage problem, thereby demonstrating its NP-hardness, as stated in [24]. \square

A.2 Proof of Proposition 3.5

To prove the existence of an optimal adversary for our hierarchical problem, we demonstrate that optimal solutions exist for both the upper-level and lower-level attackers. The optimal adversary strategy can be determined by enumerating all possible configurations for the upper-level attacker and find the optimal policy for the lower-level attacker.

Step 1: Lower-Level Attacker

For the lower-level attacker, the identities of the victim and the adversary agents are fixed. The policy of the victim agents, denoted by $\prod_{i \in \mathcal{N}} \pi_\beta(a^i | s^i, \mu)$, is also fixed. This allows us to incorporate the victim's policy into the environment's transition dynamics, resulting in a modified transition function given by:

$$p'(s'^i | s^i, a^i, \mu, \nu) = p(s'^i | s^i, a^i, \mu, \nu) \cdot \prod_{i \in \mathcal{N}} \pi_\beta(a^i | s^i, \mu).$$

The lower-level attacker thus faces a new MFC problem with these modified environment dynamics p' . According to the results established in [66], an optimal policy exists for MFC problems, ensuring that the lower-level attacker can achieve an optimal strategy.

Step 2: Upper-Level Attacker

The upper-level attacker faces a finite combinatorial problem, as it involves selecting k agents from a total of N agents, leading to $\binom{N}{k}$ possible combinations. The optimal solution can be determined by exhaustively enumerating all possible combinations of agents and evaluating the corresponding outcomes.

For each combination of agents selected by the upper-level attacker, we train an MFC policy for the lower-level attacker. Given that an optimal policy is guaranteed for the lower-level problem, each combination of upper-level selections results in a cumulative reward.

Since the upper-level problem is a finite combinatorial optimization problem, there exists an optimal solution that maximizes the cumulative reward. Thus, the optimal adversary strategy consists of the optimal set of agents selected by the upper-level attacker, combined with the optimal lower-level policy determined by the MFC problem. Therefore, an optimal adversary exists for this hierarchical problem. \square

A.3 Proof of proposition. 4.1

(1) Bound for $\hat{\pi}$.

As $\hat{\pi}^i = \epsilon^i \pi_\alpha^i + (1 - \epsilon^i) \pi_\beta^i$, we can expand $\|\hat{\pi}^i - \pi_\beta^i\|_p$ by:

$$\|\hat{\pi}^i - \pi_\beta^i\|_p = \|\epsilon^i \pi_\alpha^i + (1 - \epsilon^i) \pi_\beta^i - \pi_\beta^i\|_p = \|\epsilon^i (\pi_\alpha^i - \pi_\beta^i)\|_p = \epsilon^i \|\pi_\alpha^i - \pi_\beta^i\|_p \leq 2^{1/p} \epsilon^i. \quad (15)$$

Note that $\|\pi_\alpha^i - \pi_\beta^i\|_p \leq 2^{1/p}$. \square

(2) Bound for ν .

We first consider the case when $N \rightarrow \infty$. In this case,

$$\lim_{N \rightarrow \infty} \|\nu(a) - \nu_\beta(a)\|_p = \left\| \frac{1}{N} \sum_{i \in \mathcal{N}} (\hat{\pi}^i - \hat{\pi}_\beta^i) \right\|_p = \frac{1}{N} \left\| \sum_{i \in \mathcal{N}} (\hat{\pi}^i - \hat{\pi}_\beta^i) \right\|_p. \quad (16)$$

Applying Jensen's inequality, we have:

$$\frac{1}{N} \left\| \sum_{i \in \mathcal{N}} (\hat{\pi}^i - \hat{\pi}_\beta^i) \right\|_p \leq \frac{1}{N} \sum_{i \in \mathcal{N}} \|\hat{\pi}^i - \hat{\pi}_\beta^i\|_p \leq \frac{1}{N} \sum_{i \in \mathcal{N}} 2^{1/p} \epsilon^i = 2^{1/p} \xi. \quad (17)$$

Next, for finite N ,

$$p \left(\left| \|\nu(a) - \nu_\beta(a)\|_p - \mathbb{E}[\|\nu(a) - \nu_\beta(a)\|_p] \right| \geq \delta \right) \quad (18)$$

$$= p \left(\left| \frac{1}{N} \sum_{i \in \mathcal{N}} \delta(a^i = a | \hat{\pi}^i) - \delta(a^i = a | \pi_\beta^i) \right|_p - 2^{1/p} \xi \right| \geq \delta \right) \quad (\text{By Eqn. 17}) \quad (19)$$

$$\leq p \left(\left| \frac{1}{N} \sum_{i \in \mathcal{N}} \|\delta(a^i = a | \hat{\pi}^i) - \delta(a^i = a | \pi_\beta^i)\|_p - 2^{1/p} \xi \right| \geq \delta \right) \quad (\text{By Jensen's equality}). \quad (20)$$

Since $\delta(a^i = a | \hat{\pi}^i)$ and $\delta(a^i = a | \pi_\beta^i) \in \{0, 1\}$, we have each independent variable $\frac{1}{N} \|\delta(a^i = a | \hat{\pi}^i) - \delta(a^i = a | \pi_\beta^i)\|_p \leq \frac{1}{N}$. Thus, by Hoeffding's inequality, $\forall \delta > 0$,

$$p \left(\left| \frac{1}{N} \sum_{i \in \mathcal{N}} \|\delta(a^i = a | \hat{\pi}^i) - \delta(a^i = a | \pi_\beta^i)\|_p - 2^{1/p} \xi \right| \geq \delta \right) \quad (21)$$

$$\leq 2 \exp \left(- \frac{2\delta^2}{\sum_{i \in \mathcal{N}} (1/N)^2} \right) = 2 \exp(-2N\delta^2) \quad (22)$$

To sum up, we have

$$p \left(\left| \|\nu(a) - \nu_\beta(a)\|_p - 2^{1/p} \xi \right| \geq \delta \right) \leq 2 \exp(-2N\delta^2), \quad \forall \delta > 0. \quad (23)$$

This completes the proof. \square

A.4 Proof of Proposition. 4.2

We begin our proof from Eqn. 10, using $\hat{\pi}_\alpha^i = \hat{\pi}^i - \pi_\beta^i$ as a shorthand, such that the perturbation budget is bounded by $\hat{\pi}_\alpha^i$ directly:

$$\begin{aligned}
& \max_{\pi_\alpha \in \mathcal{A}} V^i(s^i, \mu) - (\mathcal{B}^{\hat{\pi}} V^i)(s^i, \mu), \\
&= \max_{\pi_\alpha \in \mathcal{A}} V^i(s^i, \mu) - \sum_{a^i, a \in \mathcal{A}} (\hat{\pi}_\alpha^i + \pi_\beta^i) (\hat{\nu}_\alpha(a) + \nu_\beta(a)) \left[r_t + \gamma \sum_{s'^i \in \mathcal{S}} p(s'^i | s^i, a^i, \mu, \nu) V^i(s'^i, \mu') \right] \\
&= \max_{\|\hat{\pi}_\alpha^i\|_p \leq \epsilon^i, \|\hat{\nu}_\alpha\|_p \leq \xi} V^i(s^i, \mu) - \sum_{a^i, a \in \mathcal{A}} (\hat{\pi}_\alpha^i + \pi_\beta^i) (\hat{\nu}_\alpha(a) + \nu_\beta(a)) \left[r_t \right. \\
&\quad \left. + \gamma \sum_{s'^i \in \mathcal{S}} p(s'^i | s^i, a^i, \mu, \nu) V^i(s'^i, \mu') \right] \\
&= \max_{\|\hat{\pi}_\alpha^i\|_p \leq \epsilon^i, \|\hat{\nu}_\alpha\|_p \leq \xi} V^i(s^i, \mu) - \sum_{a^i, a \in \mathcal{A}} (\hat{\pi}_\alpha^i \hat{\nu}_\alpha(a) + \hat{\pi}_\alpha^i \nu_\beta(a) + \pi_\beta^i \hat{\nu}_\alpha(a) + \pi_\beta^i \nu_\beta(a)) \left[r_t \right. \\
&\quad \left. + \gamma \sum_{s'^i \in \mathcal{S}} p(s'^i | s^i, a^i, \mu, \nu) V^i(s'^i, \mu') \right] \\
&= V^i(s^i, \mu) - \max_{\|\hat{\pi}_\alpha^i\|_p \leq \epsilon^i, \|\hat{\nu}_\alpha\|_p \leq \xi} \sum_{a^i, a \in \mathcal{A}} \hat{\pi}_\alpha^i \hat{\nu}_\alpha(a) \left[r + \gamma \sum_{s'^i \in \mathcal{S}} p(s'^i | s^i, a^i, \mu, \nu) V^i(s'^i, \mu') \right] \\
&\quad - \max_{\|\hat{\pi}_\alpha^i\|_p \leq \epsilon^i} \sum_{a^i, a \in \mathcal{A}} \hat{\pi}_\alpha^i \nu_\beta(a) \left[r + \gamma \sum_{s'^i \in \mathcal{S}} p(s'^i | s^i, a^i, \mu, \nu) V^i(s'^i, \mu') \right] \\
&\quad - \max_{\|\hat{\nu}_\alpha\|_p \leq \xi} \sum_{a^i, a \in \mathcal{A}} \hat{\pi}_\beta^i \nu_\alpha(a) \left[r + \gamma \sum_{s'^i \in \mathcal{S}} p(s'^i | s^i, a^i, \mu, \nu) V^i(s'^i, \mu') \right] \\
&\quad - \sum_{a^i, a \in \mathcal{A}} \hat{\pi}_\beta^i \nu_\beta(a) \left[r + \gamma \sum_{s'^i \in \mathcal{S}} p(s'^i | s^i, a^i, \mu, \nu) V^i(s'^i, \mu') \right].
\end{aligned}$$

Since the equation is too long, we analyze each separately. For the first line, we have:

$$\begin{aligned}
& \max_{\|\hat{\pi}_\alpha^i\|_p \leq \epsilon^i, \|\hat{\nu}_\alpha\|_p \leq \xi} \sum_{a^i, a \in \mathcal{A}} \hat{\pi}_\alpha^i \hat{\nu}_\alpha(a) \left[r + \gamma \sum_{s'^i \in \mathcal{S}} p(s'^i | s^i, a^i, \mu, \nu) V^i(s'^i, \mu') \right] \\
&= \max_{\hat{\pi}_\alpha^i \in \mathcal{A}, \hat{\nu}_\alpha \in \mathcal{A}} \sum_{a^i, a \in \mathcal{A}} \hat{\pi}_\alpha^i \hat{\nu}_\alpha(a) \left[r + \gamma \sum_{s'^i \in \mathcal{S}} p(s'^i | s^i, a^i, \mu, \nu) V^i(s'^i, \mu') \right] \\
&= \max_{\hat{\pi}_\alpha^i \in \mathcal{A}, \hat{\nu}_\alpha \in \mathcal{A}} \sum_{a^i, a \in \mathcal{A}} (\hat{\pi}_\alpha^i \hat{\nu}_\alpha(a) + \delta_{\|\hat{\pi}_\alpha^i\|_p \leq \epsilon^i, \|\hat{\nu}_\alpha\|_p \leq \xi}) \left[r + \gamma \sum_{s'^i \in \mathcal{S}} p(s'^i | s^i, a^i, \mu, \nu) V^i(s'^i, \mu') \right]. \\
&= - \min_{\hat{\pi}_\alpha^i \in \mathcal{A}, \hat{\nu}_\alpha \in \mathcal{A}} \sum_{a^i, a \in \mathcal{A}} (\hat{\pi}_\alpha^i \hat{\nu}_\alpha(a) + \delta_{\|\hat{\pi}_\alpha^i\|_p \leq \epsilon^i, \|\hat{\nu}_\alpha\|_p \leq \xi}) \left[r + \gamma \sum_{s'^i \in \mathcal{S}} p(s'^i | s^i, a^i, \mu, \nu) V^i(s'^i, \mu') \right].
\end{aligned}$$

We can write it in the form needed by Fenchel-Rockafellar transform:

$$\begin{aligned}
& - \min_{\hat{\pi}_\alpha^i \in \mathcal{A}, \hat{\nu}_\alpha \in \mathcal{A}} \sum_{a^i, a \in \mathcal{A}} (\hat{\pi}_\alpha^i \hat{\nu}_\alpha(a) + \delta_{\|\hat{\pi}_\alpha^i\|_p \leq \epsilon^i, \|\hat{\nu}_\alpha\|_p \leq \xi}) \left[r + \gamma \sum_{s'^i \in \mathcal{S}} p(s'^i | s^i, a^i, \mu, \nu) V^i(s'^i, \mu') \right] \\
&= - \min_{\hat{\pi}_\alpha^i \in \mathcal{A}, \hat{\nu}_\alpha \in \mathcal{A}} \langle \hat{\pi}_\alpha^i \hat{\nu}_\alpha, r + \gamma \sum_{s'^i \in \mathcal{S}} p(s'^i | s^i, a^i, \mu, \nu) V^i(s'^i, \mu') \rangle \\
&\quad + \langle \delta_{\|\hat{\pi}_\alpha^i\|_p \leq \epsilon^i, \|\hat{\nu}_\alpha\|_p \leq \xi}, r + \gamma \sum_{s'^i \in \mathcal{S}} p(s'^i | s^i, a^i, \mu, \nu) V^i(s'^i, \mu') \rangle
\end{aligned}$$

We can then apply Fenchel-Rockafellar transform:

$$f^*(-y) = \max_{\hat{\pi}_\alpha^i \in \mathcal{A}, \hat{\nu}_\alpha \in \mathcal{A}} -\langle \hat{\pi}_\alpha^i \hat{\nu}_\alpha, y \rangle - \langle \hat{\pi}_\alpha^i \hat{\nu}_\alpha, r + \gamma \sum_{s' \in \mathcal{S}} p(s'^i | s^i, a^i, \mu, \nu) V^i(s'^i, \mu') \rangle.$$

To maximize the following objective, we have:

$$y = -(r^i + \gamma \sum_{s' \in \mathcal{S}} p(s'^i | s^i, a^i, \mu, \nu) V^i(s'^i, \mu')) = -Q^i(s^i, a^i, \mu, \nu).$$

Plugging in y , we get:

$$\begin{aligned} & - \min_{\hat{\pi}_\alpha^i \in \mathcal{A}, \hat{\nu}_\alpha \in \mathcal{A}} \langle \hat{\pi}_\alpha^i \hat{\nu}_\alpha, r + \gamma \sum_{s' \in \mathcal{S}} p(s'^i | s^i, a^i, \mu, \nu_\beta) V^i(s'^i, \mu') \rangle \\ & \quad + \langle \delta \| \hat{\pi}_\alpha^i \|_p \leq \epsilon^i, \| \hat{\nu}_\alpha \|_p \leq \xi, r + \gamma \sum_{s' \in \mathcal{S}} p(s'^i | s^i, a^i, \mu, \nu) V^i(s'^i, \mu') \rangle \\ & = \langle \delta \| \hat{\pi}_\alpha^i \|_p \leq \epsilon^i, \| \hat{\nu}_\alpha \|_p \leq \xi, Q^i(s^i, a^i, \mu, \nu) \rangle \\ & = \epsilon^i \xi \| Q^i(s^i, a^i, \mu, \nu) \|_q. \end{aligned}$$

Similar to this derivation, other equations in our expanded form can be written as:

$$\begin{aligned} & \max_{\| \hat{\pi}_\alpha^i \|_p \leq \epsilon^i} \sum_{a^i \in \mathcal{A}} \hat{\pi}_\alpha^i \nu_\beta(a) \left[r + \gamma \sum_{s' \in \mathcal{S}} p(s'^i | s^i, a^i, \mu, \nu) V^i(s'^i, \mu') \right] \\ & = \epsilon^i \| Q^i(s^i, a^i, \mu, \nu) \|_q. \end{aligned}$$

and

$$\begin{aligned} & \max_{\| \nu_\alpha \|_p \leq \xi} \sum_{a^i \in \mathcal{A}} \hat{\pi}_\beta^i \nu_\alpha(a) \left[r + \gamma \sum_{s' \in \mathcal{S}} p(s'^i | s^i, a^i, \mu, \nu) V^i(s'^i, \mu') \right] \\ & = \xi \| Q^i(s^i, a^i, \mu, \nu) \|_q \end{aligned}$$

Note that the derivation processes are mostly the same, so we do not waste space on writing these very similar derivations.

Summing all these together, we get:

$$\begin{aligned} & \max_{\pi_\alpha \in \mathcal{A}} V^i(s^i, \mu) - (\mathcal{B}^{\hat{\pi}} V^i)(s^i, \mu) \\ & = V^i(s^i, \mu) - \sum_{a^i \in \mathcal{A}} \hat{\pi}_\beta^i \nu_\beta(a) \left[r + \gamma \sum_{s' \in \mathcal{S}} p(s'^i | s^i, a^i, \mu, \nu) V^i(s'^i, \mu') \right] + (\epsilon^i + \xi + \epsilon^i \xi) \| Q^i(s^i, a^i, \mu, \nu) \|_q \\ & = V^i(s^i, \mu) - (\mathcal{B}^{\pi_\beta} V^i)(s^i, \mu) + (\epsilon^i + \xi + \epsilon^i \xi) \| Q^i(s^i, a^i, \mu, \nu) \|_q. \end{aligned}$$

This completes the proof. \square

A.5 Proof of Proposition. 4.3

Given the Bellman equation $\mathcal{B}_{\epsilon^i, \xi}^R V^i(s^i, \mu, \epsilon^i, \xi) = (\mathcal{B}^{\pi_\beta} V^i)(s^i, \mu) + (\epsilon^i + \xi + \epsilon^i \xi) \| Q^i(s^i, a^i, \mu, \nu) \|_q$, let $V_1^i, V_2^i \in \mathbb{R}^{|\mathcal{S} \times \mathcal{S} \times [0,1] \times [0,1]|}$. Consider any $s \in \mathcal{S}, \mu \in \mathcal{S}, \epsilon^i \in [0, 1], \xi \in [0, 1]$, we have:

$$\begin{aligned} & | \mathcal{B}_{\epsilon^i, \xi}^R V_1^i(s^i, \mu, \epsilon^i, \xi) - \mathcal{B}_{\epsilon^i, \xi}^R V_2^i(s^i, \mu, \epsilon^i, \xi) | \\ & = | (\mathcal{B}^{\pi_\beta} V_1^i)(s^i, \mu) + (\epsilon^i + \xi + \epsilon^i \xi) \| Q^i(s^i, a^i, \mu, \nu) \|_q - (\mathcal{B}^{\pi_\beta} V_2^i)(s^i, \mu) - (\epsilon^i + \xi + \epsilon^i \xi) \| Q^i(s^i, a^i, \mu, \nu) \|_q | \\ & = | (\mathcal{B}^{\pi_\beta} V_1^i)(s^i, \mu) - (\mathcal{B}^{\pi_\beta} V_2^i)(s^i, \mu) |. \end{aligned}$$

Here, $\| Q^i(s^i, a^i, \mu, \nu) \|_q$ term cancels out each other since it is defined as the Q function under the benign transition, which can be learned in the benign mean-field game and is not involved in the learning process of $\mathcal{B}_{\epsilon^i, \xi}^R V^i(s^i, \mu, \epsilon^i, \xi)$. Thus, $\mathcal{B}^{\pi_\beta} V^i(s^i, \mu)$ is the transition under benign policy π_β .

The Bellman operator $\mathcal{B}^{\pi_\beta} V^i$ can be written as:

$$\mathcal{B}^{\pi_\beta} V^i(s^i, \mu) = \sum_{a \in \mathcal{A}} \pi_\beta(a^i | s^i, \mu) \nu(a) \left[r + \gamma \sum_{s' \in \mathcal{S}} p(s'^i | s^i, a^i, \mu, \nu) V(s'^i, \mu') \right]$$

Thus, the proof proceeds by:

$$\begin{aligned}
& |\mathcal{B}_{\epsilon^i, \xi}^R V_1^i(s^i, \mu, \epsilon^i, \xi) - \mathcal{B}_{\epsilon^i, \xi}^R V_2^i(s^i, \mu, \epsilon^i, \xi)| \\
&= |(\mathcal{B}^{\pi_\beta} V_1^i)(s^i, \mu) - (\mathcal{B}^{\pi_\beta} V_2^i)(s^i, \mu)| \\
&= \left| \sum_{a \in \mathcal{A}} \pi_\beta(a^i | s^i, \mu) \nu(a) \left[r + \gamma \sum_{s' \in \mathcal{S}} p(s'^i | s^i, a^i, \mu, \nu) V_2^i(s'^i, \mu') \right] - \right. \\
&\quad \left. \sum_{a \in \mathcal{A}} \pi_\beta(a^i | s^i, \mu) \nu(a) \left[r + \gamma \sum_{s' \in \mathcal{S}} p(s'^i | s^i, a^i, \mu, \nu) V_2^i(s'^i, \mu') \right] \right| \\
&= \left| \sum_{a \in \mathcal{A}} \pi_\beta(a^i | s^i, \mu) \nu(a) \gamma \sum_{s' \in \mathcal{S}} p(s'^i | s^i, a^i, \mu, \nu) (V_1^i(s'^i, \mu') - V_2^i(s'^i, \mu')) \right| \\
&\leq \gamma \sum_{a \in \mathcal{A}} \pi_\beta(a^i | s^i, \mu) \nu(a) \sum_{s' \in \mathcal{S}} p(s'^i | s^i, a^i, \mu, \nu) |V_1^i(s'^i, \mu') - V_2^i(s'^i, \mu')| \\
&= \gamma |V_1^i(s^i, \mu') - V_2^i(s^i, \mu')|
\end{aligned}$$

This completes the proof. \square

A.6 Proof for Proposition. 4.4

First, we apply first-order linear approximation to Q function under $\hat{\pi}$, $Q_{\hat{\pi}}^i(s^i, a^i, \mu, \nu)$. Similar to proof of A.4, we use $\hat{\pi}_\alpha^i = \hat{\pi}^i - \pi_\beta^i$ as a shorthand, resulting in:

$$Q_{\hat{\pi}}^i(s^i, a^i, \mu, \nu) = Q_{\pi_\beta}^i(s^i, a^i, \mu, \nu) + \min_{\|\hat{\pi}_\alpha^i\|_p \leq \epsilon^i, \|\nu_\alpha\|_p \leq \xi} \sum_{a^i, a \in \mathcal{A}} \hat{\pi}_\alpha \nu_\alpha Q_{\pi_\beta}^i(s^i, a^i, \mu, \nu).$$

Using Hölder's Inequality, we have:

$$\left\| \min_{\|\hat{\pi}_\alpha^i\|_p \leq \epsilon^i, \|\nu_\alpha\|_p \leq \xi} \sum_{a^i, a \in \mathcal{A}} \hat{\pi}_\alpha \nu_\alpha Q_{\pi_\beta}^i(s^i, a^i, \mu, \nu) \right\|_1 \leq \|\hat{\pi}_\alpha^i\|_p \|\nu_\alpha\|_p \|Q_{\pi_\beta}^i(s^i, a^i, \mu, \nu)\|_q,$$

with minimum achieved when $\hat{\pi}_\alpha^i$ and ν_α aligns negatively with $Q_{\pi_\beta}^i(s^i, a^i, \mu, \nu)$, i.e.,

$$\hat{\pi}_\alpha^i \nu_\alpha = -\epsilon^i \xi \frac{Q_{\pi_\beta}^i(s^i, a^i, \mu, \nu)^{q-1}}{\|Q_{\pi_\beta}^i(s^i, a^i, \mu, \nu)\|_q^{q-1}}.$$

Using this worst-case $\hat{\pi}_\alpha^i \nu_\alpha$, we get:

$$\begin{aligned}
\left\| \min_{\|\hat{\pi}_\alpha^i\|_p \leq \epsilon^i, \|\nu_\alpha\|_p \leq \xi} \sum_{a^i, a \in \mathcal{A}} \hat{\pi}_\alpha \nu_\alpha Q_{\pi_\beta}^i(s^i, a^i, \mu, \nu) \right\|_1 &= \|\hat{\pi}_\alpha^i\|_p \|\nu_\alpha\|_p \|Q_{\pi_\beta}^i(s^i, a^i, \mu, \nu)\|_q \\
&= \epsilon^i \xi \|Q_{\pi_\beta}^i(s^i, a^i, \mu, \nu)\|_q
\end{aligned}$$

We omit π_β in $Q_{\pi_\beta}^i$ in our main text for conciseness. This completes the proof. \square

A.7 Proof of Proposition. 4.5

We prove the optimal solution $\mathcal{K}^* \subseteq \mathcal{N}$ and π_α^* of HAD-MFC $\mathcal{G} := \langle \mathcal{N}, \mathcal{S}, \mathcal{A}, \mathcal{P}, R, \mu_0, \nu_0, \gamma \rangle$ is the same as the optimal solution $\mathcal{K}_{\mathcal{M}}^*$ of the upper-level MDP $\mathcal{M} := \langle \mathcal{S}, \epsilon, \mathcal{N}, \tilde{\mathcal{P}}, \tilde{R}, \gamma \rangle$ with reward defined in Eqn. 13, and the value $V^{i,*}(s^i, \mu, \epsilon^i, \xi)$ of lower-level problem is learned by regularized mean-field Bellman operator $\mathcal{B}_{\epsilon^i, \xi}^R$, and learning a lower-level worst-case adversarial policy π_α^* on $\mathcal{K}_{\mathcal{M}}^*$.

First, the lower-level problem requires calculating $\min_{\pi_\alpha} J(\pi_\alpha, \pi_\beta)$. In Proposition. 4.2, by Rockafellar-Fenchel transform, we have shown that:

$$\begin{aligned} \max_{\pi_\alpha} V^i(s^i, \mu) - (\hat{\mathcal{B}}^{\hat{\pi}} V^i)(s^i, \mu) &= V^i(s^i, \mu) - \mathcal{B}_{\epsilon^i, \xi}^R V^i(s^i, \mu, \epsilon^i, \xi) \\ &= V^i(s^i, \mu) - (\mathcal{B}^{\pi_\beta} V^i)(s^i, \mu) + (\epsilon^i + \xi + \epsilon^i \xi) \|Q^i(s^i, a^i, \mu, \nu)\|_q, \end{aligned} \quad (24)$$

where $(\hat{\mathcal{B}}^{\hat{\pi}} V^i)(s^i, \mu)$ refers to the Bellman operator with the worst-case adversary. Rockafellar-Fenchel transform holds when the uncertainty set is convex, proper, and lower semi-continuous. This is satisfied by our rectangular p-norm bounded uncertainty set, as shown by the proof in Proposition. 4.1. Hence, the transform yields the exact optimal value of the original lower-level problem. Here, Rockfellar-Fenchel transform requires the convexity of the uncertainty set only, and do not require the value function or the policy to be convex.

Second, for the optimality of the upper-level MDP $\mathcal{M} := \langle \mathcal{S}, \epsilon, \mathcal{N}, \tilde{\mathcal{P}}, \tilde{R}, \gamma \rangle$, the reward in Eqn. 13 is defined on the optimal value of the lower-level problem. By Bellman's theorem [67], there exists an optimal policy for the MDP that maximizes the expected cumulative reward. Thus, solving this MDP yields the optimal solution $\mathcal{K}_{\mathcal{M}}^* \subseteq \mathcal{N}$ for the upper-level, which is also the optimal solution $\mathcal{K}^* \subseteq \mathcal{N}$ of HAD-MFC.

Finally, for the lower-level problem, since the high-level vulnerable agent selection yields the same result, the lower-level problem face the mean-field MARL problem with same transition dynamics and same group of victims. Thus, the lower-level problem yields the same lower-level optimal policy π_α . \square

B Algorithm details

Our VAI algorithm involves a multi-step approach. In step 1, we evaluate the value function using regularized mean-field Bellman operator $\mathcal{B}_{\epsilon^i, \xi}^R$. In step 2, we solve the upper-level problem by training an RL algorithm to sequentially identify the most vulnerable agents, resulting in a set of vulnerable agents. Finally, in step 3, we train an adversarial policy on these identified vulnerable agents using MFC.

Step 1. In this step, we evaluate the value function $V^i(s^i, \mu, \epsilon^i, \xi)$ via regularized mean-field Bellman operator $\mathcal{B}_{\epsilon^i, \xi}^R$. The input is a set of trajectories sampled from a cooperative MFC policy. Note that we assume shared V^i and Q^i for all agents.

Step 2. In this step, we train an RL agent to sequentially identify the most vulnerable agent. In our paper, we train this agent via Q-learning [68]. Otherwise, we use a greedy algorithm to identify the most vulnerable agents. We hereby propose both our VAI-RL and VAI-greedy algorithm.

The third and final step is to solve the lower-level problem, *i.e.*, train a zero-sum, worst-case adversarial policy on the selected set \mathcal{K} . This can be done by any standard MFC algorithm. In our algorithm, we use MF-AC [1] with shared reward as an example.

C Experiment details

C.1 Environment details

We evaluate our algorithm on three environments: Magent, Vicsek, and Taxi. Visualizations of these environments are provided in Fig. 3.

Magent. The Magent platform [6] supports large-scale multi-agent reinforcement learning with tasks such as pursuit, battle, combined arms, and tiger deer. We test our algorithm on pursuit and battle. In

Algorithm 1 Step 1: computing value function $V^i(s^i, \mu, \epsilon^i, \xi)$.

Input: Trajectories τ_β sampled from cooperative policy π_β .

Output: Trained value function $V^i(s^i, \mu, \epsilon^i, \xi)$ via regularized mean-field Bellman operator $\mathcal{B}_{\epsilon^i, \xi}^R$.

```

1: // Estimate  $Q^i$  without perturbation
2: for Iterations Iter = 0, 1, 2, ... K do
3:   for Minibatch  $\tau$  in trajectories  $\tau_\beta$  do
4:     Extract  $[s, a, \mu, \nu, r, s', a', \mu', \nu']$  from  $\tau$ .
5:     Compute  $Q^i(s^i, a^i, \mu, \nu)$  and  $Q^i(s'^i, a'^i, \mu', \nu')$ 
6:     Update  $Q^i$  by minimizing  $(\gamma Q^i(s'^i, a'^i, \mu', \nu') + r - Q^i(s^i, a^i, \mu, \nu))^2$ .
7:   end for
8: end for
9: // Estimate  $V^i$  with perturbation
10: for Iterations Iter = 0, 1, 2, ... K do
11:   for Minibatch  $\tau$  in trajectories  $\tau_\beta$  do
12:     for Sample  $i = 0, 1, 2, \dots B$  do
13:       Extract  $[s^i, a^i, \mu, \nu, r, s'^i, a'^i, \mu', \nu']$  from  $\tau_i$ .
14:       Sample  $\xi^i \sim Uniform[0, 1]$ ,  $\epsilon^i \sim Bernouli(\xi)$ .
15:       Compute  $V^i(s^i, \mu, \epsilon^i, \xi^i)$  and  $V^i(s'^i, \mu', \epsilon^i, \xi^i)$ .
16:       Compute  $Q^i(s'^i, a'^i, \mu', \nu')$  using estimated  $Q^i$  from  $\tau_\beta$ .
17:       Compute  $\min_{\|a_\alpha^i\|_p \leq \epsilon^i, \|\nu'_\alpha\|_p \leq \xi^i} \|Q^i(s'^i, (a_\beta^i + a_\alpha^i), \mu', (\nu'_\beta + \nu'_\alpha))\|_q$ ,
18:       Update  $V^i$  using Eqn. 14.
19:     end for
20:   end for
21: end for

```

Algorithm 2 Step 2: Vulnerable Agent Identification, using Q learning (VAI-RL).

Input: Q function for vulnerable agent identification $Q(s, \epsilon, n)$, trained value function $V^i(s, \mu, \epsilon^i, \xi)$.

Output: Trained Q function for vulnerable agent identification $Q(s, \epsilon, n)$, set of vulnerable agents \mathcal{K} .

```

1: Initialize vulnerable agent identification policy  $Q(s, \epsilon, n)$ ,  $\mathcal{K} = \emptyset$ ,  $\epsilon_0 = \{0\}_N$ .
2: for Episode = 0, 1, 2, ... E do
3:   for k = 1, 2, ... K do
4:     Perform rollout under  $n_k = \arg \max_{n \in \mathcal{N}} Q^n(s_k^n, \epsilon_k^n, \xi_k)$ , update  $\epsilon_k, \xi_k$ .
5:      $\mathcal{K} \leftarrow \mathcal{K} \cup n_k$ .
6:     Compute  $V^i(s, \mu, \epsilon^i, \xi)$  for all agents.
7:     Compute reward  $r_k = \frac{1}{N} \sum_{i \in \mathcal{N}} (V^i(s_0^i, \mu_0, \epsilon_k^i, \xi_k) - V^i(s_0^i, \mu_0, \epsilon_{k-1}^i, \xi_{k-1}))$  following Eqn. 13.
8:   end for
9:   Save tuple  $\langle s_k, \epsilon_k, n_k, r_k \rangle$  in replay buffer.
10:  Update  $Q(s, \epsilon, n)$  via DQN.
11: end for

```

pursuit, red agents navigate obstacles to tag blue agents, while the blue agents evade. Our method identifies vulnerable red agents. In battle, agents engage in large-scale combat, earning rewards based on performance. We focus on the left-side agents for vulnerability identification.

Taxi. The Taxi supply-demand matching environment [8] allows agents to control taxis, receiving partial observations of their location and neighboring zones. A global reward is given for maintaining an optimal ratio of available taxis to demand in each zone.

Vicsek. The Vicsek model [63] simulates collective motion in flocks, where agents adjust their direction based on neighbors. We test both the original rule-based model and our modified MFC-based version, where agents follow a policy to maximize directional agreement.

Algorithm 3 Step 2: Vulnerable Agent Identification, using greedy algorithm (VAI-Greedy).

Input: Trained value function $V^i(s, \mu, \epsilon^i, \xi)$.

Output: Set of vulnerable agents \mathcal{K} .

```
1: Initialize  $\mathcal{K} = \emptyset, \epsilon_0 = \{0\}_N$ .
2: for  $k = 1, 2, \dots, K$  do
3:   for  $i = 1, 2, \dots, N$  do
4:      $r_k^{max} = -\infty, n_k^{max} = 1$ .
5:     if  $n_k^i \in \mathcal{K}$  then
6:       pass
7:     else
8:       Perform rollout under  $n_k^i$ , compute  $\epsilon_k^i, \xi_k$ .
9:       Compute  $V^i(s, \mu, \epsilon^i, \xi)$  for all agents.
10:      Compute reward  $r_k = \frac{1}{N} \sum_{i \in \mathcal{N}} (V^i(s_0^i, \mu_0, \epsilon_k^i, \xi_k) - V^i(s_0^i, \mu_0, \epsilon_{k-1}^i, \xi_{k-1}))$  following Eqn. 13.
11:      end if
12:      if  $r_k \geq r_k^{max}$  then
13:         $r_k^{max} \leftarrow r_k, n_k^{max} \leftarrow n_k^i$ .
14:         $\mathcal{K} \leftarrow \mathcal{K} \cup n_k^i$ .
15:      end if
16:    end for
17: end for
```

Algorithm 4 Step 3: Learning the Adversarial Policy for Lower-Level Problem.

Input: Adversarial policy π_α , victim policy π_β , set of vulnerable agents \mathcal{K} , perturbation budget ϵ^i .

Output: Trained adversarial policy π_α .

```
1: Initialize vulnerable agent identification policy  $\pi^{VAI}, \mathcal{K} = \emptyset$ .
2: for Episode = 0, 1, 2, ... E do
3:   for  $t = 1, 2, \dots, T$  do
4:     Get  $s_t^i, \mu$  from environment.
5:     Compute  $\hat{\pi}^i(a_t^i | s_t^i, \mu) = \epsilon^i \pi_\alpha^i(\cdot | s_t^i, \mu) + (1 - \epsilon^i) \pi_\beta^i(a_t^i | s_t^i, \mu)$  for all  $i \in \mathcal{N}$ .
6:     Sample  $a_t^i \sim \hat{\pi}^i(\cdot | s_t^i, \mu)$ . Compute  $\nu$ .
7:     Calculate  $r_t$  from environment.
8:     Store  $[s_t^i, a_t^i, \mu_t, \nu_t, r_t]$  in trajectory  $\tau$ .
9:   end for
10:  for  $k = 0, 1, \dots, K$  do
11:    Sample a batch  $\tau_k$  from trajectory  $\tau$ .
12:    Update the critic  $Q^i(s_i, a_i, \mu, \nu)$  by minimizing TD loss  $(\gamma Q^i(s^i, a^i, \mu', \nu') + r - Q^i(s^i, a^i, \mu, \nu))^2$ .
13:    Update the policy of adversary  $\pi_\alpha$  by sampled policy gradient  $-\nabla_{\pi_\alpha} \log \pi_\alpha Q^i(s^i, a^i, \mu, \nu)$ .
14:  end for
15: end for
```

C.2 Implementation Details

Our implementation builds upon the mean-field MARL framework introduced by [1]. For the baseline implementations, as our environment lacks an inherent graph structure, we construct the adjacency matrix using the following heuristic: if one agent can observe another, we assign an undirected edge between them with a weight of 1, forming an undirected graph. In the bi-level RL baseline, both input and output follow the same structure as our VAI-RL method, but rewards for the upper level are provided only after all agents are selected, and the lower-level adversarial policies are executed. The upper-level and lower-level attackers share the same reward. For PIANO, we use a graph embedding network to process the adjacency matrix and jointly train it alongside PPO for the upper-level attack. Since the setting of PIANO does not require learning an adversarial policy, the upper-level attacker's reward is defined by the reward received by lower-level attackers executing a random policy. As for RTCA, we follow the original methodology, tuning the implementation for optimal performance.

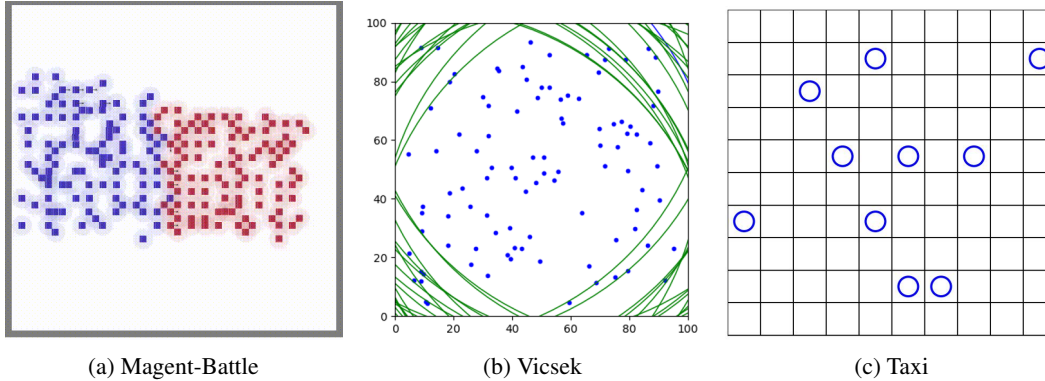


Figure 3: Environments used in our experiments. The task Battle in Magent are proposed in [6]. The Taxi environment follows [8]. Vicsek model follows the dynamics defined by [63].

Detailed descriptions of our VAI method and baseline implementations are provided in Appendix B, with hyperparameter settings in Appendix C.3.

C.3 Hyperparameters

In this section, we list all hyperparameters used Battle, Taxi and Vicsek environment. All hyperparameters are shared by VAI and other baselines. The hyperparameters used by Battle is at Table. 2.

Table 2: Hyperparameters for Battle environment.

Hyperparameter	Value	Hyperparameter	Value
agent	64/144	mapsize	40/60
adv. num	12.5/25/50%	save_every	5
n_round	2000/5000	maxsteps	400
gamma	0.95	lr	1e-4
tau	0.005	batch_size	64
memory_size	80000		

The hyperparameters used by Taxi is at Table. 3.

Table 3: Hyperparameters for Taxi environment.

Hyperparameter	Value	Hyperparameter	Value
optimizer	Adam	number of agents N	50/100
PPO clip	0.2	hidden dim	0.99
number of adv agents M	4/16/36	critic loss coefficient c_1	0.5
map size	10×10	maximum number of policy training episodes	$2 \cdot 10^6$
entropy loss coefficient c_2	0.01	data_chunk_length	10
entropy_coef	0.01	eorder num	100
actor learning rate	$3 \cdot 10^{-5}$	discount factor γ	0.99
gae_lambda	0.95	gain	0.01
gamma	0.99	hidden_sizes	[128, 128]
order price	1/2	update every E episodes	5
batch size	64	length of an episode T	20

The hyperparameters used by Vicsek is at Table. 4.

Table 4: Hyperparameters for Vicsek environment.

Hyperparameter	Value	Hyperparameter	Value
action_aggregation	prod	activation_func	relu
actor_num_mini_batch	1	clip_param	0.05
critic_epoch	5	critic_lr	0.0005
critic_num_mini_batch	1	cuda	true
cuda_deterministic	true	data_chunk_length	10
entropy_coef	0.01	episode_length	200
eval_episodes	20	eval_interval	25
gae_lambda	0.95	gain	0.01
gamma	0.99	hidden_sizes	[128, 128]
huber_delta	10.0	initialization_method	orthogonal_
world_size	100	log_interval	5
lr	0.0005	max_grad_norm	10.0
torus	true	n_eval_rollout_threads	10
n_rollout_threads	5	num_env_steps	5000000
opti_eps	1e-05	ppo_epoch	5
recurrent_n	1	render_episodes	10
seed	1	seed_specify	true
share_param	true	std_x_coef	1
std_y_coef	0.5	torch_threads	4
use_clipped_value_loss	true	use_eval	true
use_feature_normalization	true	use_gae	true
use_huber_loss	true	use_linear_lr_decay	false
use_max_grad_norm	true	use_policy_active_masks	true
use_popart	true	use_proper_time_limits	true
use_recurrent_policy	false	use_render	false
value_loss_coef	1	weight_decay	0
use_agent_states_init	true	bearing_bins	8
comm_radius	20	distance_bins	8
dynamics	unicycle	nr_agents	100
obs_mode	fix_acc		

D Additional Result

D.1 Complexity and Runtime Efficiency

Table 5: Runtime Comparison of All Methods (in hours)

Agent Num	Adv Num	Random	DC	Bi-Level	RL	PIANO	RTCA	VAI-Greedy	VAI-RL
64	32	1.68	1.60	1.94	1.84	2.92	1.64 + 1 (V func.)	1.75 + 1 (V func.)	
144	72	3.78	3.63	4.00	4.05	5.62	3.83 + 1 (V func.)	4.28 + 1 (V func.)	

In this section, we analyze the computation cost of VAI and baselines. The overall results are shown in Table. 5. Our VAI consists of two stages. First, we train a V function using the regularized mean-field Bellman operator (Proposition 4.2). This process, which involves computing a regularization Q function, is comparable in complexity to a typical value update in mean-field MARL and takes about 1 hour. Once trained, the V function is fixed and reused across both VAI-Greedy and VAI-RL, so it is trained only once.

Second, we select the most vulnerable agents, using VAI-Greedy or VAI-RL. VAI-Greedy performs adversary selection by ranking agent vulnerabilities using the V function. It has $O(NK)$ complexity (selecting K agents from N), but incurs negligible cost in practice (<1 second for both 64 and 144 agents) since it do not requires additional training. VAI-RL uses Q-learning to sequentially select vulnerable agents. It incurs modest computation overhead: +9.4% for 64 agents and +17.9% for 144 agents compared to the best-performing baseline. Our VAI-RL is fast since it do not need interactions with the environment. Its complexity scales as $O(K)$ (number of adversaries), and can be efficiently

extended using techniques to handle large number of agents by using large-action space approximation techniques in RL [69].

As for baselines, Random and DC use simple heuristics for adversary selection and require minimal compute. Most of their time is spent training the main RL policy (about 1.6h for 64 agents, 3.6h for 144 agents). However, their performance can be inferior since they do not consider the underlying task dynamics. Bi-Level RL trains an additional high-level RL selector; PIANO trains a GNN-based selector, both introducing moderately increase cost. RTCA is the most compute-heavy baseline due to maintaining 10 evolutionary populations for adversary selection.

To summarize, while our method adds cost from training the V function, it is amortized across both VAI-Greedy and VAI-RL. Beyond that, VAI’s selection procedures are efficient, with computation time on par with or lower than several baselines (especially RTCA), making it a practical and scalable solution.

D.2 Performance with Partial Perturbation Budgets ϵ

While our main experiments focused on the extreme case of $\epsilon = 1$, assuming the attacker take complete control of the policy, we add further evaluations under partial perturbations $\epsilon = \{0.3, 0.5, 0.7\}$. We conduct all experiments on Battle environment, with 64 agents and 32 adversaries, and 144 agents with 72 adversaries. The results are presented in the Table. 6. While our VAI-RL and VAI-Greedy outperforms all baselines in general, there are several points worth analysis.

First, VAI-RL works constantly better for VAI-Greedy. With less perturbation budgets and more adversaries, the algorithms requires more fine-grained exploration to the weakness of the overall system. In this way, the results given by VAI-Greedy may be simple and less optimal. In contrast, VAI-RL can better exploit the synergy effect of adversaries, which also works better for smaller perturbation budgets.

Second, the result also shows our VAI-RL and VAI-Greedy works better in various perturbation budgets ϵ . While we observed that the impact of adversaries are generally reduced with smaller ϵ , the effect of our VAI is consistent with this constained budget.

Table 6: Performance comparison under different perturbation budgets ϵ (\downarrow).

Num Agent	Adv Agent	Method	ϵ		
			0.7	0.5	0.3
64	32	Random	167.4	198.5	191.7
		DC	137.7	155.3	184.9
		Bi-Level RL	95.4	103.8	116.1
		PIANO	77.9	94.93	107.2
		RTCA	86.9	103.2	133.8
		VAI-Greedy	74.4	83.0	92.3
		VAI-RL	55.3	78.4	79.0
144	72	Random	-115.8	92.0	276.9
		DC	-229.9	-109.5	-77.1
		Bi-Level RL	-252.2	-93.4	-62.7
		PIANO	-207.3	-93.0	-88.5
		RTCA	-298.1	-138.0	66.9
		VAI-Greedy	-338.6	-149.9	40.3
		VAI-RL	-406.3	-243.8	-151.6

NeurIPS Paper Checklist

1. Claims

Question: Do the main claims made in the abstract and introduction accurately reflect the paper's contributions and scope?

Answer: [\[Yes\]](#)

Justification: Main claims have reflected our contributions and scope.

Guidelines:

- The answer NA means that the abstract and introduction do not include the claims made in the paper.
- The abstract and/or introduction should clearly state the claims made, including the contributions made in the paper and important assumptions and limitations. A No or NA answer to this question will not be perceived well by the reviewers.
- The claims made should match theoretical and experimental results, and reflect how much the results can be expected to generalize to other settings.
- It is fine to include aspirational goals as motivation as long as it is clear that these goals are not attained by the paper.

2. Limitations

Question: Does the paper discuss the limitations of the work performed by the authors?

Answer: [\[Yes\]](#)

Justification: We have described limitations in conclusions.

Guidelines:

- The answer NA means that the paper has no limitation while the answer No means that the paper has limitations, but those are not discussed in the paper.
- The authors are encouraged to create a separate "Limitations" section in their paper.
- The paper should point out any strong assumptions and how robust the results are to violations of these assumptions (e.g., independence assumptions, noiseless settings, model well-specification, asymptotic approximations only holding locally). The authors should reflect on how these assumptions might be violated in practice and what the implications would be.
- The authors should reflect on the scope of the claims made, e.g., if the approach was only tested on a few datasets or with a few runs. In general, empirical results often depend on implicit assumptions, which should be articulated.
- The authors should reflect on the factors that influence the performance of the approach. For example, a facial recognition algorithm may perform poorly when image resolution is low or images are taken in low lighting. Or a speech-to-text system might not be used reliably to provide closed captions for online lectures because it fails to handle technical jargon.
- The authors should discuss the computational efficiency of the proposed algorithms and how they scale with dataset size.
- If applicable, the authors should discuss possible limitations of their approach to address problems of privacy and fairness.
- While the authors might fear that complete honesty about limitations might be used by reviewers as grounds for rejection, a worse outcome might be that reviewers discover limitations that aren't acknowledged in the paper. The authors should use their best judgment and recognize that individual actions in favor of transparency play an important role in developing norms that preserve the integrity of the community. Reviewers will be specifically instructed to not penalize honesty concerning limitations.

3. Theory assumptions and proofs

Question: For each theoretical result, does the paper provide the full set of assumptions and a complete (and correct) proof?

Answer: [\[Yes\]](#)

Justification: We have provided a complete set of assumptions and proofs.

Guidelines:

- The answer NA means that the paper does not include theoretical results.
- All the theorems, formulas, and proofs in the paper should be numbered and cross-referenced.
- All assumptions should be clearly stated or referenced in the statement of any theorems.
- The proofs can either appear in the main paper or the supplemental material, but if they appear in the supplemental material, the authors are encouraged to provide a short proof sketch to provide intuition.
- Inversely, any informal proof provided in the core of the paper should be complemented by formal proofs provided in appendix or supplemental material.
- Theorems and Lemmas that the proof relies upon should be properly referenced.

4. Experimental result reproducibility

Question: Does the paper fully disclose all the information needed to reproduce the main experimental results of the paper to the extent that it affects the main claims and/or conclusions of the paper (regardless of whether the code and data are provided or not)?

Answer: [Yes]

Justification: All implementations and hyperparameters are described.

Guidelines:

- The answer NA means that the paper does not include experiments.
- If the paper includes experiments, a No answer to this question will not be perceived well by the reviewers: Making the paper reproducible is important, regardless of whether the code and data are provided or not.
- If the contribution is a dataset and/or model, the authors should describe the steps taken to make their results reproducible or verifiable.
- Depending on the contribution, reproducibility can be accomplished in various ways. For example, if the contribution is a novel architecture, describing the architecture fully might suffice, or if the contribution is a specific model and empirical evaluation, it may be necessary to either make it possible for others to replicate the model with the same dataset, or provide access to the model. In general, releasing code and data is often one good way to accomplish this, but reproducibility can also be provided via detailed instructions for how to replicate the results, access to a hosted model (e.g., in the case of a large language model), releasing of a model checkpoint, or other means that are appropriate to the research performed.
- While NeurIPS does not require releasing code, the conference does require all submissions to provide some reasonable avenue for reproducibility, which may depend on the nature of the contribution. For example
 - (a) If the contribution is primarily a new algorithm, the paper should make it clear how to reproduce that algorithm.
 - (b) If the contribution is primarily a new model architecture, the paper should describe the architecture clearly and fully.
 - (c) If the contribution is a new model (e.g., a large language model), then there should either be a way to access this model for reproducing the results or a way to reproduce the model (e.g., with an open-source dataset or instructions for how to construct the dataset).
 - (d) We recognize that reproducibility may be tricky in some cases, in which case authors are welcome to describe the particular way they provide for reproducibility. In the case of closed-source models, it may be that access to the model is limited in some way (e.g., to registered users), but it should be possible for other researchers to have some path to reproducing or verifying the results.

5. Open access to data and code

Question: Does the paper provide open access to the data and code, with sufficient instructions to faithfully reproduce the main experimental results, as described in supplemental material?

Answer: [No]

Justification: Code will be released after acceptance.

Guidelines:

- The answer NA means that paper does not include experiments requiring code.
- Please see the NeurIPS code and data submission guidelines (<https://nips.cc/public/guides/CodeSubmissionPolicy>) for more details.
- While we encourage the release of code and data, we understand that this might not be possible, so “No” is an acceptable answer. Papers cannot be rejected simply for not including code, unless this is central to the contribution (e.g., for a new open-source benchmark).
- The instructions should contain the exact command and environment needed to run to reproduce the results. See the NeurIPS code and data submission guidelines (<https://nips.cc/public/guides/CodeSubmissionPolicy>) for more details.
- The authors should provide instructions on data access and preparation, including how to access the raw data, preprocessed data, intermediate data, and generated data, etc.
- The authors should provide scripts to reproduce all experimental results for the new proposed method and baselines. If only a subset of experiments are reproducible, they should state which ones are omitted from the script and why.
- At submission time, to preserve anonymity, the authors should release anonymized versions (if applicable).
- Providing as much information as possible in supplemental material (appended to the paper) is recommended, but including URLs to data and code is permitted.

6. Experimental setting/details

Question: Does the paper specify all the training and test details (e.g., data splits, hyper-parameters, how they were chosen, type of optimizer, etc.) necessary to understand the results?

Answer: [Yes]

Justification: We have described these.

Guidelines:

- The answer NA means that the paper does not include experiments.
- The experimental setting should be presented in the core of the paper to a level of detail that is necessary to appreciate the results and make sense of them.
- The full details can be provided either with the code, in appendix, or as supplemental material.

7. Experiment statistical significance

Question: Does the paper report error bars suitably and correctly defined or other appropriate information about the statistical significance of the experiments?

Answer: [No]

Justification: In RL we typically report results on 5 random seeds as well as 95% confidence.

Guidelines:

- The answer NA means that the paper does not include experiments.
- The authors should answer "Yes" if the results are accompanied by error bars, confidence intervals, or statistical significance tests, at least for the experiments that support the main claims of the paper.
- The factors of variability that the error bars are capturing should be clearly stated (for example, train/test split, initialization, random drawing of some parameter, or overall run with given experimental conditions).
- The method for calculating the error bars should be explained (closed form formula, call to a library function, bootstrap, etc.)
- The assumptions made should be given (e.g., Normally distributed errors).
- It should be clear whether the error bar is the standard deviation or the standard error of the mean.

- It is OK to report 1-sigma error bars, but one should state it. The authors should preferably report a 2-sigma error bar than state that they have a 96% CI, if the hypothesis of Normality of errors is not verified.
- For asymmetric distributions, the authors should be careful not to show in tables or figures symmetric error bars that would yield results that are out of range (e.g. negative error rates).
- If error bars are reported in tables or plots, The authors should explain in the text how they were calculated and reference the corresponding figures or tables in the text.

8. Experiments compute resources

Question: For each experiment, does the paper provide sufficient information on the computer resources (type of compute workers, memory, time of execution) needed to reproduce the experiments?

Answer: [No]

Justification: Our work do not focus on computing efficiency.

Guidelines:

- The answer NA means that the paper does not include experiments.
- The paper should indicate the type of compute workers CPU or GPU, internal cluster, or cloud provider, including relevant memory and storage.
- The paper should provide the amount of compute required for each of the individual experimental runs as well as estimate the total compute.
- The paper should disclose whether the full research project required more compute than the experiments reported in the paper (e.g., preliminary or failed experiments that didn't make it into the paper).

9. Code of ethics

Question: Does the research conducted in the paper conform, in every respect, with the NeurIPS Code of Ethics [https://neurips.cc/public/EthicsGuidelines?](https://neurips.cc/public/EthicsGuidelines)

Answer: [Yes]

Justification: We follow the ethics.

Guidelines:

- The answer NA means that the authors have not reviewed the NeurIPS Code of Ethics.
- If the authors answer No, they should explain the special circumstances that require a deviation from the Code of Ethics.
- The authors should make sure to preserve anonymity (e.g., if there is a special consideration due to laws or regulations in their jurisdiction).

10. Broader impacts

Question: Does the paper discuss both potential positive societal impacts and negative societal impacts of the work performed?

Answer: [Yes]

Justification: We have discussed them in conclusions.

Guidelines:

- The answer NA means that there is no societal impact of the work performed.
- If the authors answer NA or No, they should explain why their work has no societal impact or why the paper does not address societal impact.
- Examples of negative societal impacts include potential malicious or unintended uses (e.g., disinformation, generating fake profiles, surveillance), fairness considerations (e.g., deployment of technologies that could make decisions that unfairly impact specific groups), privacy considerations, and security considerations.
- The conference expects that many papers will be foundational research and not tied to particular applications, let alone deployments. However, if there is a direct path to any negative applications, the authors should point it out. For example, it is legitimate to point out that an improvement in the quality of generative models could be used to

generate deepfakes for disinformation. On the other hand, it is not needed to point out that a generic algorithm for optimizing neural networks could enable people to train models that generate Deepfakes faster.

- The authors should consider possible harms that could arise when the technology is being used as intended and functioning correctly, harms that could arise when the technology is being used as intended but gives incorrect results, and harms following from (intentional or unintentional) misuse of the technology.
- If there are negative societal impacts, the authors could also discuss possible mitigation strategies (e.g., gated release of models, providing defenses in addition to attacks, mechanisms for monitoring misuse, mechanisms to monitor how a system learns from feedback over time, improving the efficiency and accessibility of ML).

11. Safeguards

Question: Does the paper describe safeguards that have been put in place for responsible release of data or models that have a high risk for misuse (e.g., pretrained language models, image generators, or scraped datasets)?

Answer: [NA]

Justification: This is a theoretical paper.

Guidelines:

- The answer NA means that the paper poses no such risks.
- Released models that have a high risk for misuse or dual-use should be released with necessary safeguards to allow for controlled use of the model, for example by requiring that users adhere to usage guidelines or restrictions to access the model or implementing safety filters.
- Datasets that have been scraped from the Internet could pose safety risks. The authors should describe how they avoided releasing unsafe images.
- We recognize that providing effective safeguards is challenging, and many papers do not require this, but we encourage authors to take this into account and make a best faith effort.

12. Licenses for existing assets

Question: Are the creators or original owners of assets (e.g., code, data, models), used in the paper, properly credited and are the license and terms of use explicitly mentioned and properly respected?

Answer: [Yes]

Justification: We have cited them.

Guidelines:

- The answer NA means that the paper does not use existing assets.
- The authors should cite the original paper that produced the code package or dataset.
- The authors should state which version of the asset is used and, if possible, include a URL.
- The name of the license (e.g., CC-BY 4.0) should be included for each asset.
- For scraped data from a particular source (e.g., website), the copyright and terms of service of that source should be provided.
- If assets are released, the license, copyright information, and terms of use in the package should be provided. For popular datasets, paperswithcode.com/datasets has curated licenses for some datasets. Their licensing guide can help determine the license of a dataset.
- For existing datasets that are re-packaged, both the original license and the license of the derived asset (if it has changed) should be provided.
- If this information is not available online, the authors are encouraged to reach out to the asset's creators.

13. New assets

Question: Are new assets introduced in the paper well documented and is the documentation provided alongside the assets?

Answer: [NA]

Justification: We do not release new assets.

Guidelines:

- The answer NA means that the paper does not release new assets.
- Researchers should communicate the details of the dataset/code/model as part of their submissions via structured templates. This includes details about training, license, limitations, etc.
- The paper should discuss whether and how consent was obtained from people whose asset is used.
- At submission time, remember to anonymize your assets (if applicable). You can either create an anonymized URL or include an anonymized zip file.

14. **Crowdsourcing and research with human subjects**

Question: For crowdsourcing experiments and research with human subjects, does the paper include the full text of instructions given to participants and screenshots, if applicable, as well as details about compensation (if any)?

Answer: [NA]

Justification: The paper does not involve crowdsourcing nor research with human subjects

Guidelines:

- The answer NA means that the paper does not involve crowdsourcing nor research with human subjects.
- Including this information in the supplemental material is fine, but if the main contribution of the paper involves human subjects, then as much detail as possible should be included in the main paper.
- According to the NeurIPS Code of Ethics, workers involved in data collection, curation, or other labor should be paid at least the minimum wage in the country of the data collector.

15. **Institutional review board (IRB) approvals or equivalent for research with human subjects**

Question: Does the paper describe potential risks incurred by study participants, whether such risks were disclosed to the subjects, and whether Institutional Review Board (IRB) approvals (or an equivalent approval/review based on the requirements of your country or institution) were obtained?

Answer: [NA]

Justification: The paper does not involve crowdsourcing nor research with human subjects.

Guidelines:

- The answer NA means that the paper does not involve crowdsourcing nor research with human subjects.
- Depending on the country in which research is conducted, IRB approval (or equivalent) may be required for any human subjects research. If you obtained IRB approval, you should clearly state this in the paper.
- We recognize that the procedures for this may vary significantly between institutions and locations, and we expect authors to adhere to the NeurIPS Code of Ethics and the guidelines for their institution.
- For initial submissions, do not include any information that would break anonymity (if applicable), such as the institution conducting the review.

16. **Declaration of LLM usage**

Question: Does the paper describe the usage of LLMs if it is an important, original, or non-standard component of the core methods in this research? Note that if the LLM is used only for writing, editing, or formatting purposes and does not impact the core methodology, scientific rigor, or originality of the research, declaration is not required.

Answer: [NA]

Justification: We polish writing only.

Guidelines:

- The answer NA means that the core method development in this research does not involve LLMs as any important, original, or non-standard components.
- Please refer to our LLM policy (<https://neurips.cc/Conferences/2025/LLM>) for what should or should not be described.